

Fusion Reactor Technology I

(459.760, 3 Credits)

Prof. Dr. Yong-Su Na

(32-206, Tel. 880-7204)

Contents

Week 1. Magnetic Confinement

Week 2. Fusion Reactor Energetics (Harms 2, 7.1-7.5)

Week 3. Tokamak Operation (I):

Basic Tokamak Plasma Parameters (Wood 1.2, 1.3)

Week 4. Tokamak Operation (II): Startup

Week 5. Tokamak Operation (III): Tokamak Operation Mode

Week 7-8. Tokamak Operation Limits (I):

Plasma Instabilities (Kadomtsev 6, 7, Wood 6)

Week 9-10. Tokamak Operation Limits (II):

Plasma Transport (Kadomtsev 8, 9, Wood 3, 4)

Week 11. Heating and Current Drive (Kadomtsev 10)

Week 12. Divertor and Plasma-Wall Interaction

Week 13-14. How to Build a Tokamak (Dendy 17 by T. N. Todd)

Contents

Week 1. Magnetic Confinement

Week 2. Fusion Reactor Energetics (Harms 2, 7.1-7.5)

Week 3. Tokamak Operation (I):

Basic Tokamak Plasma Parameters (Wood 1.2, 1.3)

Week 4. Tokamak Operation (II): Startup

Week 5. Tokamak Operation (III): Tokamak Operation Mode

Week 7-8. Tokamak Operation Limits (I):

Plasma Instabilities (Kadomtsev 6, 7, Wood 6)

Week 9-10. Tokamak Operation Limits (II):

Plasma Transport (Kadomtsev 8, 9, Wood 3, 4)

Week 11. Heating and Current Drive (Kadomtsev 10)

Week 12. Divertor and Plasma-Wall Interaction

Week 13-14. How to Build a Tokamak (Dendy 17 by T. N. Todd)

Stability

- Energy Principle

$$\omega^2 = \frac{\delta W}{K} \geq 0 \quad \text{stable}$$

$$\delta W \geq 0 \quad \text{stable}$$

$$\delta W = \delta W_F + \delta W_S + \delta W_V$$

$$\delta W_F = \frac{1}{2} \int_P d\vec{r} \left[\frac{|\vec{Q}|^2}{\mu_0} - \xi_{\perp}^* \cdot (\vec{J} \times \vec{Q}) + \gamma p |\nabla \cdot \xi|^2 + (\xi_{\perp} \cdot \nabla p) \nabla \cdot \xi_{\perp}^* \right]$$

$$\delta W_S = \frac{1}{2} \int_S d\vec{S} |\vec{n} \cdot \xi_{\perp}|^2 \vec{n} \cdot [[\nabla(p + B^2 / 2\mu_0)]]$$

$$\delta W_V = \frac{1}{2} \int_V d\vec{r} \frac{|\hat{B}_1|^2}{\mu_0}$$

Boundary conditions on trial functions

$$\vec{n} \cdot \hat{B}_1 \Big|_{r_w} = 0 \quad \vec{n} \cdot \hat{B}_1 \Big|_{r_p} = \hat{B}_1 \cdot \nabla (\vec{n} \cdot \xi_{\perp}) - (\vec{n} \cdot \xi_{\perp}) [\vec{n} \cdot (\vec{n} \cdot \nabla) \hat{B}_1] \Big|_{r_p}$$

Stability

• The Intuitive Form of δW_F

$$\delta W_F = \frac{1}{2} \int_P d\vec{r} \left[\underbrace{\frac{|\vec{Q}_\perp|^2}{\mu_0} + \frac{B^2}{\mu_0} |\nabla \cdot \xi_\perp + 2\xi_\perp \cdot \vec{k}|^2}_{\text{stabilising}} + \underbrace{\gamma p |\nabla \cdot \xi|^2 - 2(\xi_\perp \cdot \nabla p)(\vec{k} \cdot \xi_\perp^*) - J_\parallel (\xi_\perp^* \times \vec{b}) \cdot \vec{Q}_\perp}_{\text{destabilising}} \right]$$

Energy required to bend magnetic field lines: dominant potential energy contribution to the shear Alfvén wave
 ↓
 Energy necessary to compress the magnetic field: major potential energy contribution to the compressional Alfvén wave
 ↓
 Energy required to compress the plasma: main source of potential energy for the sound wave

Tokamak Stability

- Considering plasma states which are not in perfect thermodynamic equilibrium (no exact Maxwellian distribution, e.g. non-uniform density), even though they represent equilibrium states in the sense that the force balance is equal to 0 and a stationary solution exists, means their entropy is not at the maximum possible and hence free energy appears available which can excite perturbations to grow:
unstable equilibrium state
- The gradients of plasma current magnitude and pressure are the destabilising forces in connection with the bad magnetic field curvature

Tokamak Instabilities

- **Macroscopic MHD instabilities**

- **Ideal MHD instabilities**

- current driven (kink) instabilities
 - internal modes
 - external modes
- pressure driven instabilities
 - interchange modes
 - ballooning modes
- current+pressure driven: edge localised modes (ELMs)
- vertical instability

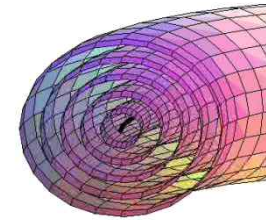
- **Resistive MHD instabilities**

- current driven instabilities
 - tearing modes
 - neoclassical tearing modes (NTMs)

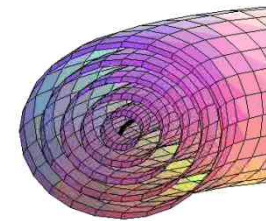
- **Nonlinear modes**

- sawtooth
- disruption

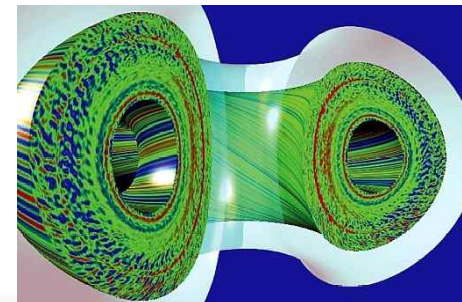
- **Microinstabilities - Transport**



Flux conservation
Topology unchanged



Reconnection of field lines
Topology changed



Classification of MHD Instabilities

- **Internal/Fixed Boundary Modes** $\vec{n} \cdot \vec{\xi} \Big|_{S_p} = 0$

- Mode structure does not require any motion of the plasma-vacuum interface away from its equilibrium position
- Singular surface ($\mathbf{B} \cdot \nabla = 0$) inside the plasma
- δW_F only needed to be considered ($\delta W_S = \delta W_V = 0$)

- **External/Free-Boundary Modes** $\vec{n} \cdot \vec{\xi} \Big|_{S_p} \neq 0$

- plasma-vacuum interface moving from its equilibrium position during an unstable MHD perturbation
- Singular surface in the vacuum region

Classification of MHD Instabilities

- **Current-Driven Modes**

- Driven by parallel currents and can exist even with $\nabla p = 0$
- Often known as “kink” modes
- The most unstable one: Internal modes with long parallel wavelengths and macroscopic perpendicular wavelengths $k_{\perp} a \sim 1$

- **Pressure-Driven Modes**

- Driven by perpendicular currents
- The most unstable one: Internal modes with very short wavelengths perpendicular to the magnetic field but long wavelengths parallel to the field

Stability

- **MHD modes**

- Normal modes of perturbation of 'straightened out' torus (standing wave)

$$\xi = \xi_0 e^{i[(k_\theta \cdot l_\theta + k_\phi \cdot l_\phi) - \omega t]} = \xi_0 e^{i\left(\frac{m}{r} \cdot r\theta - \frac{n}{R} \cdot R\phi\right)} e^{\gamma t} = \xi_0 e^{i(m\theta - n\phi)} e^{\gamma t}$$

Periodic boundary conditions:

$$k_\theta = \frac{2\pi}{\lambda_\theta} = \frac{m}{r}, \quad k_\phi = \frac{2\pi}{\lambda_\phi} = -\frac{n}{R}$$

$$\Leftrightarrow 2\pi r = m\lambda_\theta, \quad 2\pi R = -n\lambda_\phi$$

ξ : displacement of the plasma away from its equilibrium position

m, n : poloidal, toroidal mode number

γ : growth rate

The choice of a negative sign being simply for convenience

- Resonance surface

$$\vec{k} \cdot \vec{B} \equiv \frac{mB_\theta}{r} - \frac{nB_\phi}{R} = \frac{B_\theta}{r} (m - nq(r)) = 0 \Rightarrow q(r) \equiv \frac{rB_\phi}{RB_\theta(r)} = \frac{m}{n}$$

HW: why $\mathbf{k} \cdot \mathbf{B} = 0$ when the perturbation can be resonant?

Ideal MHD Instabilities

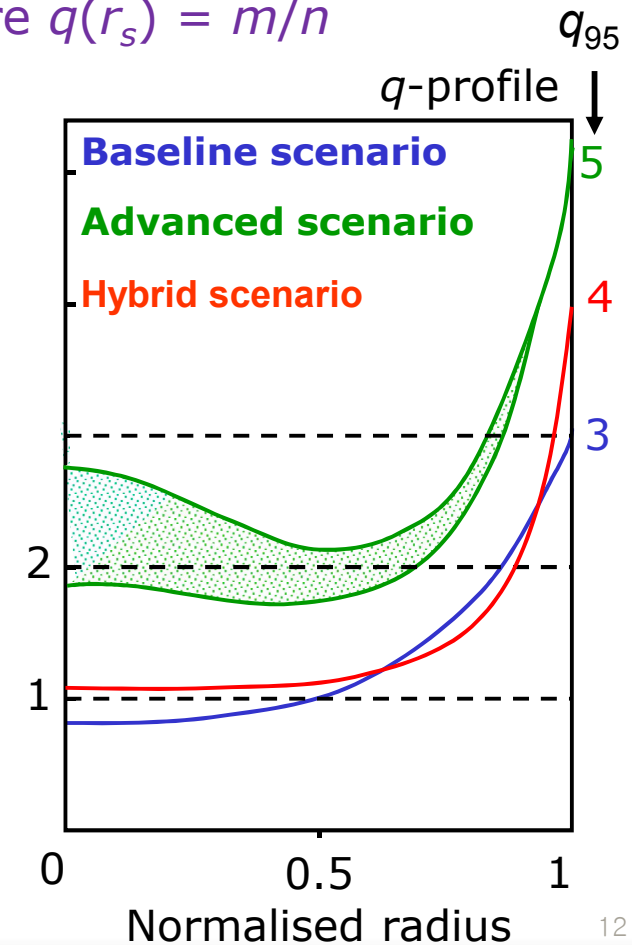
- **The most Virulent Instabilities**
 - fast growth (microseconds)
 - the possible extension over the entire plasma

Ideal MHD Instabilities

- **Internal Kink Modes**

- fixed boundary modes
- localised near rational surface $r = r_s$ where $q(r_s) = m/n$
($\mathbf{k} \cdot \mathbf{B} = 0$ for resonance)
- stability condition for $m = 1, n = 1$ mode

$$q_0 > 1$$



Ideal MHD Instabilities

- **External Kink Modes**

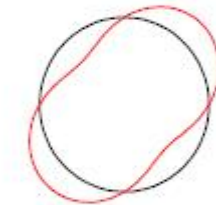
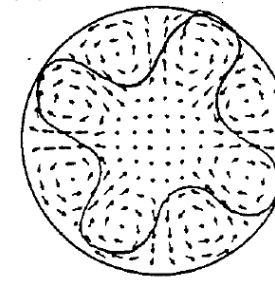
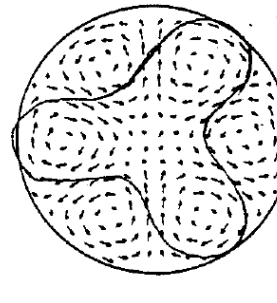
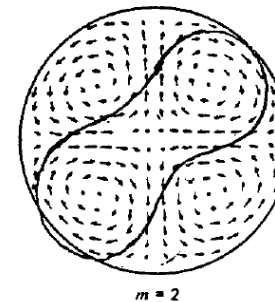
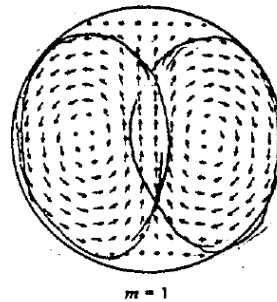
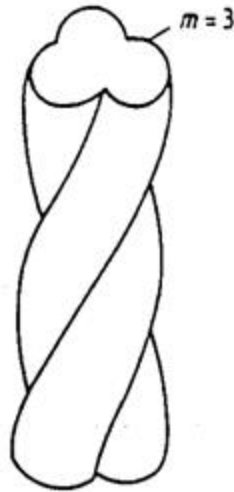
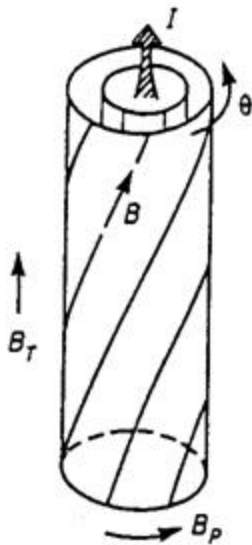
- free surface modes

- ($m = 0$ sausage, $m = 1$ helical kink, $m = 2, 3, \dots$ surface kinks)

- localised near rational surface $r = r_s$ where $q(r_s) = m/n$

- (m, n) modes fall on plasma surface $r = a$ (vacuum region):
mode rational surface $q(a) = m/n$

- fastest and most dangerous



Ideal MHD Instabilities

- **External Kink Modes**

- **Stabilising effects and stability conditions**

- conducting wall stabilisation for low n modes

- strong toroidal magnetic field

- $q(a) > m/n$ for (m, n) modes w/o conducting wall

- Kruskal-Shafranov limit for $m = n = 1$ mode

Ideal MHD Instabilities

- $m = n = 1$ external kink mode: Kruskal-Shafranov limit

In the limit where the conducting wall moves to infinity

$$\frac{\delta W_2}{W_0} = \xi_0^2 \left(n - \frac{1}{q_a} \right) \left[\left(n - \frac{1}{q_a} \right) + \left(n + \frac{1}{q_a} \right) \right] = 2\xi_0^2 \left[n \left(n - \frac{1}{q_a} \right) \right]$$

$q_a > 1$ Kruskal-Shafranov criterion:
stability condition for the $m = 1$ external kink mode
for the worst case, $n = 1$

Imposing an important constraint on tokamak operation:
toroidal current upper limit ($I < I_{KS}$)

$$I_{KS} \equiv 2\pi a^2 B_\phi(R_0) / \mu_0 R_0 = 5a^2 B_\phi(R_0) / R_0 \text{ [MA]}$$

$$q_a = \frac{aB_\phi(R_0)}{R_0 B_p} = \frac{aB_\phi(R_0)}{R_0 \mu_0 I_{KS} / 2\pi a} = 1$$

Ideal MHD Instabilities

- **External Kink Modes**

- **Stabilising effects and stability conditions**

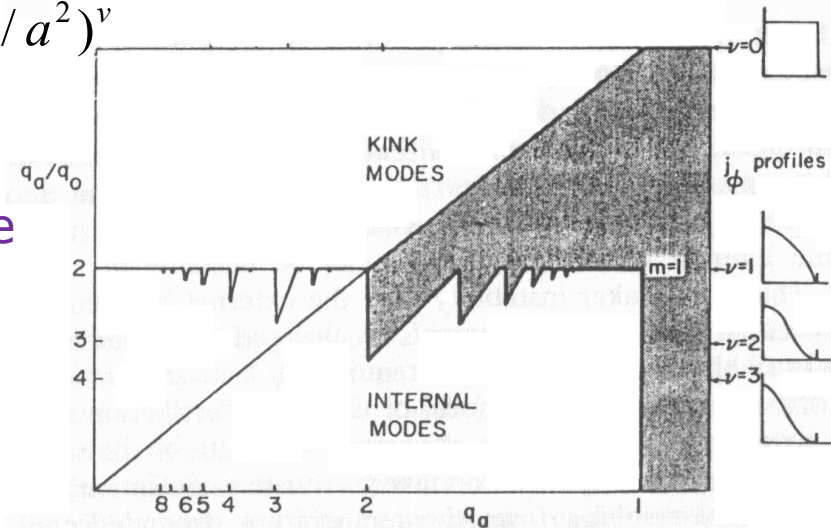
- conducting wall stabilisation for low n modes
 - strong toroidal magnetic field
 - $q(a) > m/n$ for (m, n) modes w/o conducting wall
 - Kruskal-Shafranov limit for $m = n = 1$ mode
 - centrally peaked toroidal current density profile for $m \geq 2$

$$\frac{q_a}{q_0} \geq \nu + 1 \approx 2 - 3 \text{ for } J_\phi = J_0(1 - r^2/a^2)^\nu$$

for $\nu = 0$ (uniform), always unstable against any (m, n) mode

- strong magnetic shear

$$s(r) \equiv \frac{r}{q} \frac{dq}{dr}$$



Ideal MHD Instabilities

- **Interchange Modes**

- Interchange perturbations do not grow in normal tokamaks if $q \geq 1$.
- locally grow in the outboard bad curvature region: ballooning modes
- internal modes: localised near rational surface $r = r_s$ where
$$q(r_s) = m/n$$
- no threat to confinement unless $q(0) \ll 1$

- **Interchange Modes**

- **Stabilising effects and stability conditions**

- minimum- B configuration
- magnetic shear
- Mercier necessary condition
- elongated outward triangular cross section

Ideal MHD Instabilities

- Internal localised interchange instabilities: Mercier criterion

$$\frac{d}{dx} \left(x^2 \frac{d\xi}{dx} \right) + D_s \xi = 0 \quad \begin{array}{l} \text{Straight tokamak:} \\ \text{Euler-Lagrange equation} \end{array}$$

$$\xi = x^p$$

$$p(p+1) + D_s = 0$$

$$p_{1,2} = -\frac{1}{2} \pm \frac{1}{2} (1 - 4D_s)^{1/2}$$

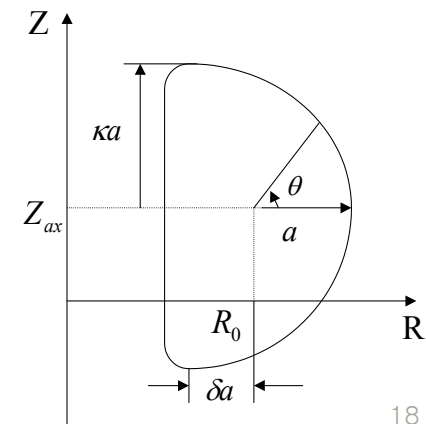
$$\left(\frac{rq'}{q} \right)^2 + \frac{8\mu_0 r p'}{B_\phi^2} > 0 \quad \begin{array}{l} \text{Suydam's} \\ \text{criterion} \end{array}$$

For a circular cross section, large aspect ratio with $\beta_p \sim 1$

$$\left(\frac{rq'}{q} \right)^2 + 4r\beta'(1 - q^2) > 0 \quad \begin{array}{l} \text{Mercier} \\ \text{criterion} \end{array} \quad q_0 > 1$$

For a non-circular cross section

$$1 < q_0^2 \left\{ 1 - \frac{4}{1 + 3\kappa^2} \left[\frac{3\kappa^2 - 1}{4\kappa^2 + 1} \left(\kappa^2 - \frac{2\delta}{\varepsilon} \right) + \frac{(\kappa - 1)^2 \beta_{p0}}{\kappa(\kappa + 1)} \right] \right\}$$



Ideal MHD Instabilities

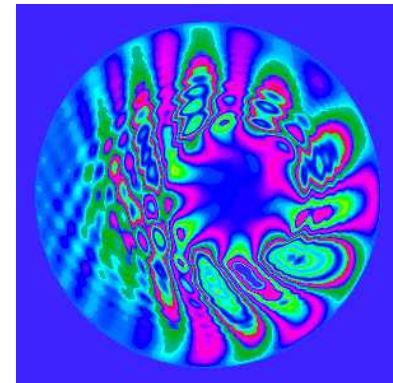
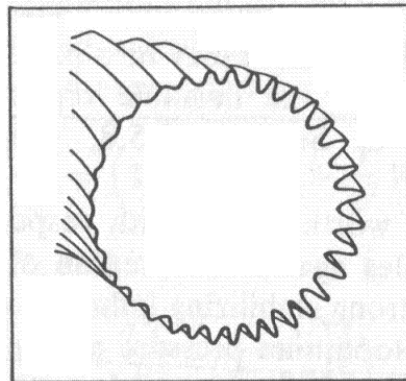
- **Ballooning Modes**

- driven by the pressure gradient at bad-curvature surface region
- localised high- n interchange mode at outbound edge of circular high- β tokamak or at the tips of an elongated plasma
- most dangerous and limiting MHD instability

- **Ballooning Modes**

- Stabilising effects and stability conditions**

- keep $\beta < \beta_{\max} \approx \epsilon/q^2$
- strong magnetic shear
- noncircular plasma shape
- conducting wall



Ideal MHD Instabilities

- Analytic model

$$\frac{\partial}{\partial \theta} \left[(1 + \Lambda^2) \frac{\partial X}{\partial \theta} \right] + \alpha (\Lambda \sin \theta + \cos \theta) X = 0$$

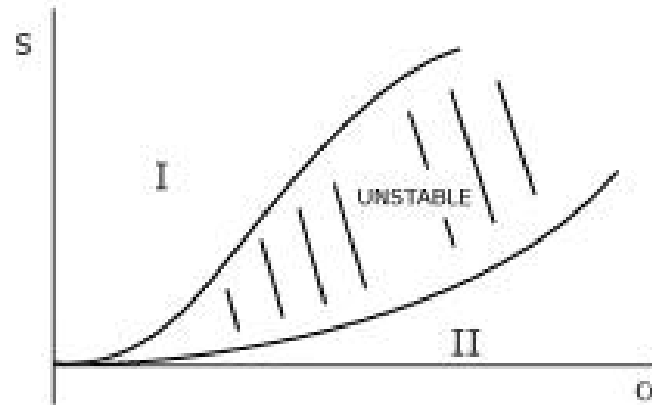
desired form of the ballooning mode equation for the model equilibrium (s, a)

$$\Lambda(\theta) = s(\theta - \theta_0) - \alpha(\sin \theta - \sin \theta_0)$$

$$s = \frac{rq'}{q} \quad \text{average shear}$$

$$\alpha = -\frac{2\mu_0 r^2 p'}{R_0 B_\theta^2} = -\frac{r^2 B_0^2}{R_0^2 B_\theta^2} \cdot R_0 \cdot \frac{p'}{B_0^2 / 2\mu_0} = -q^2 R_0 \beta'$$

measure of the pressure gradient



(s, a) diagram

Ideal MHD Instabilities

- **Numerical Results: the Sykes Limit, the Troyon Limit**

Once an equilibrium is established, the following stability tests are made.

- (1) Mercier stability
- (2) High- n ballooning modes
- (3) Low- n internal modes
- (4) External ballooning-kink modes

- Helpful in the design of new experiments and in the interpretation and analysis of existing experimental data
- Playing a role in the determination of optimised configurations
- Quantitative predictions for the maximum β_t or I_0 and that can be stably maintained in MHD equilibrium

$$\text{Troyon limit } \beta_t(\%) = \beta_N \frac{I_\phi(MA)}{a(m)B_\phi(R_0)(T)}$$

Ideal MHD Instabilities

- Limit on β due to ideal MHD instabilities

$$\begin{aligned}\beta &= \frac{p}{B^2 / 2\mu_0} \approx \beta_p \left(\frac{B_\theta}{B_\phi} \right)^2 = \beta_p \left(\frac{a / R_0}{q(a)} \right)^2 \\ &= \underbrace{\left(\frac{a}{R_0} \beta_p \right)}_{(1)} \underbrace{\left(\frac{a}{R_0} \right)}_{(2)} \underbrace{\left(\frac{q(0)}{q(a)} \right)^2}_{(3)} \underbrace{\left(\frac{1}{q(0)} \right)^2}_{(4)}\end{aligned}$$

(1) ≤ 1 : ballooning mode limit

(2) $\leq 1/3$: space limit (geometry, shielding, maintenance, heating, etc)

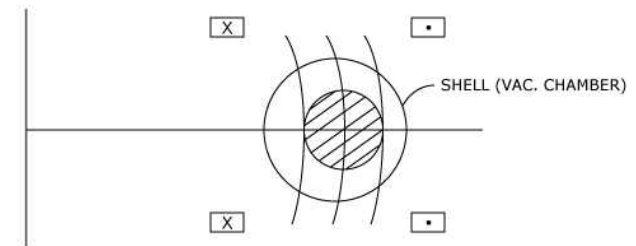
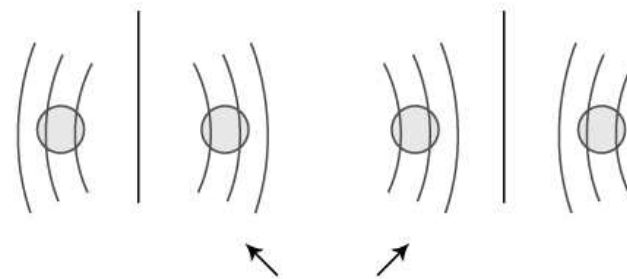
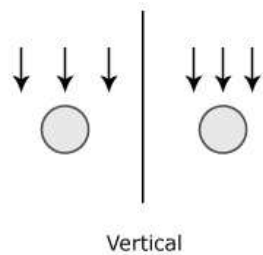
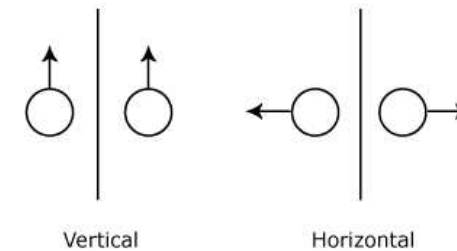
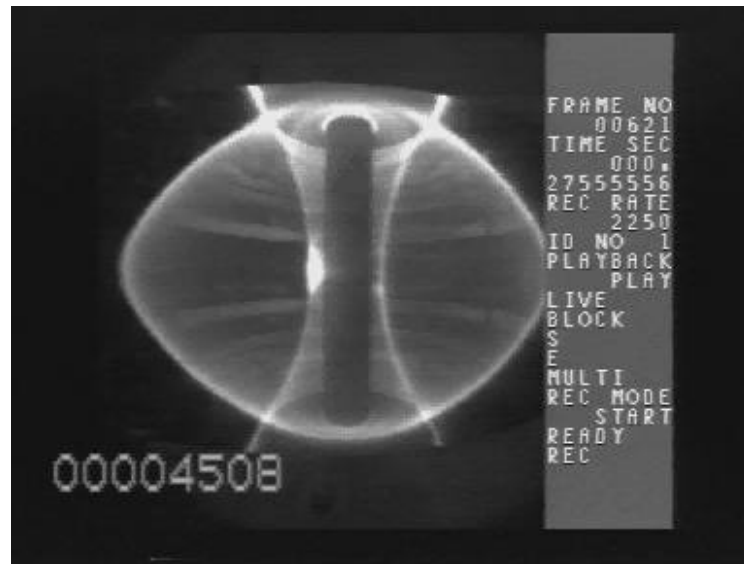
(3) ≤ 0.2 : surface kinks

(4) ≤ 1 : internal modes

Ideal MHD Instabilities

- **Vertical Instability**

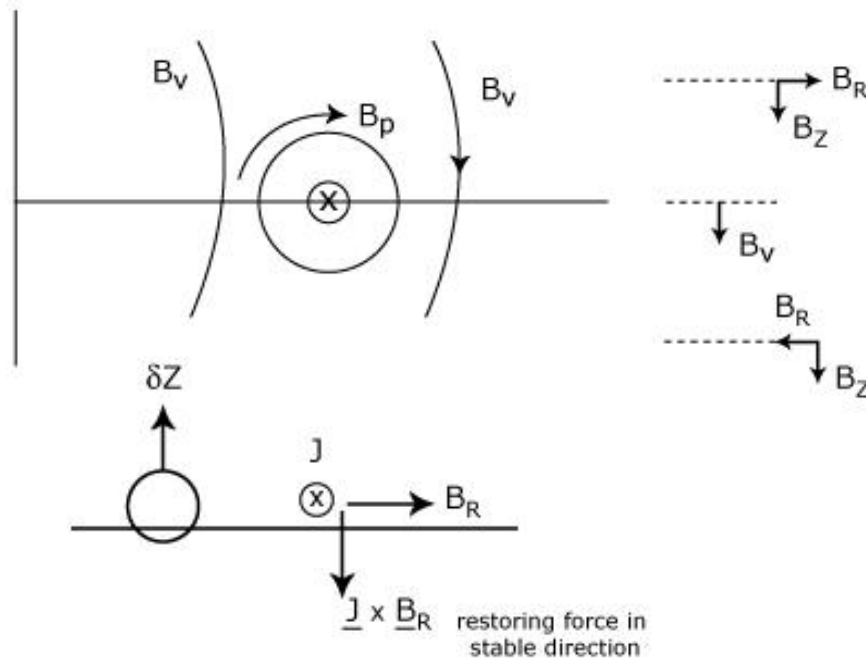
- $n = 0$ axisymmetric modes:
macroscopic motion of the plasma towards the wall



Ideal MHD Instabilities

• Vertical Instability

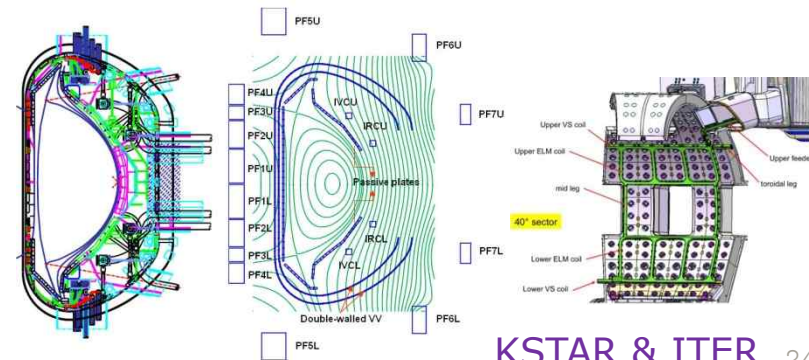
- For a circular cross sections a moderate shaping of the vertical field should provide stability.
- For noncircular tokamaks, vertical instabilities produce important limitations on the maximum achievable elongations.
- Even moderate elongations require a conducting wall or a feedback system for vertical stability.



field index

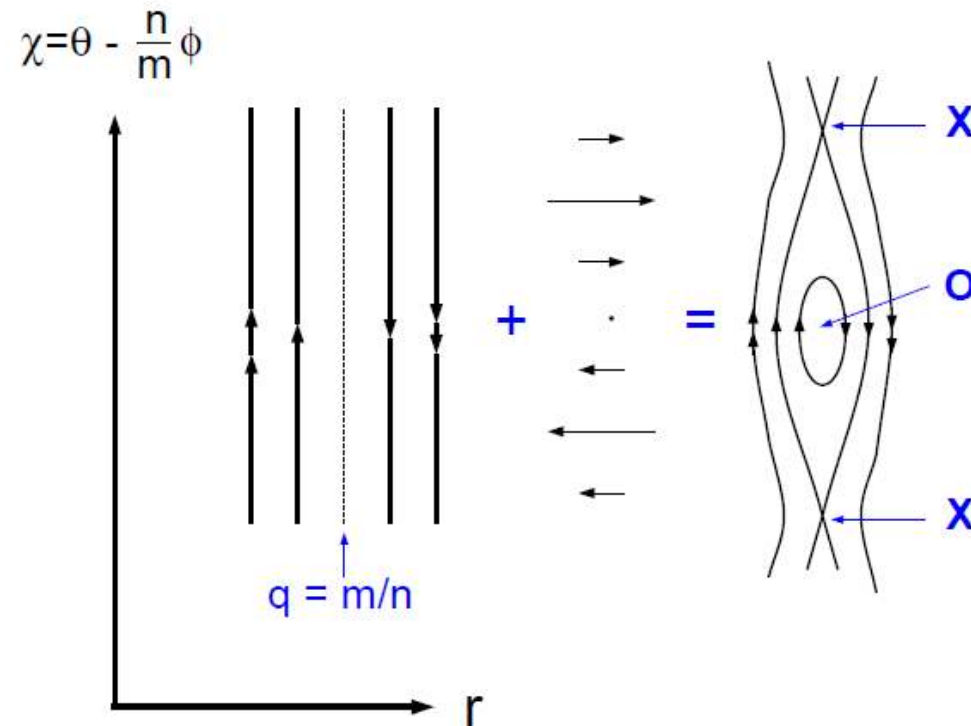
$$n(R_0, Z_0) = - \left(\frac{R}{B_Z} \frac{\partial B_Z}{\partial R} \right)_{R_0, Z_0}$$

$$0 < n < 3/2$$



Resistive MHD Instabilities

- growing more slowly compared with the ideal instabilities (10^{-4} - 10^{-2} s)
- resulting from the diffusion or tearing of the magnetic field lines relative to the plasma fluid
- destroying the nested topology of the magnetic flux surfaces

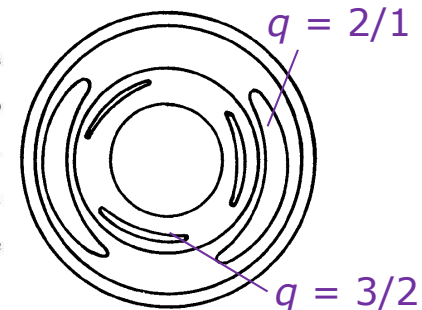
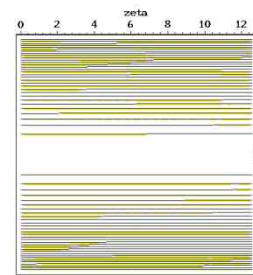


H. P. Furth et al, "Finite-Resistivity Instabilities of a Sheet Pinch" *Phys. Fluids* **6**, 459 (1963)

Resistive MHD Instabilities

- **Tearing Modes**

- resistive internal kink modes ($m \geq 2$)
- driven by perturbed \mathbf{B} induced by current layer (∇J) in plasmas
- magnetic island formation
- mode rational surface $r = r_s$ where $q(r_s) = m/n$ falls in plasmas
- saturation at some fraction of plasma width (\sim a few tenth of plasma radius a)
- growth rate $\gamma \propto \eta^{1/3}$
- more tolerable and lower than ideal modes



- **Tearing Modes**

- **Stabilising effects and stability conditions**

- unstable region reduced as sharpness of the current profile ν increases
- m increases
- closeness of the wall to the plasma
- $q(a)/q(0)$ (shear) increases

- stability condition: $q_0 > 3$

Microinstabilities

- often associated with non-Maxwellian velocity distributions: deviation from thermodynamic equilibrium (nonuniformity, anisotropy of distributions) → free energy source which can drive instabilities
- kinetic approach required: limited MHD approach
- driving anomalous transports
- **Two-stream or beam-plasma instability**
 - Particle bunching → \mathbf{E} perturbation → bunching↑ → unstable
- **Drift (or Universal) instability**
 - driven by ∇p (or ∇n) in magnetic field
 - excited by drift waves with a phase velocity of v_{De} with a very short wavelength
 - most unstable, dominant for anomalous transport
 - stabilisation: good curvature (min- \mathbf{B}), shear, finite β
- **Trapped particle modes**
 - anisotropy due to passing particles having large $v_{||}$ among trapped ones
 - Preferably when the perturbation frequency < bounce frequency
 - increasing cross-field diffusion
 - drift instability enhanced by trapped particle effects
 - Trapped Electron Mode (TEM), Trapped Ion Mode (TIM)

Non-linear Plasma Activity

• Sawtooth

VOLUME 33, NUMBER 20

PHYSICAL REVIEW LETTERS

11 NOVEMBER 1974

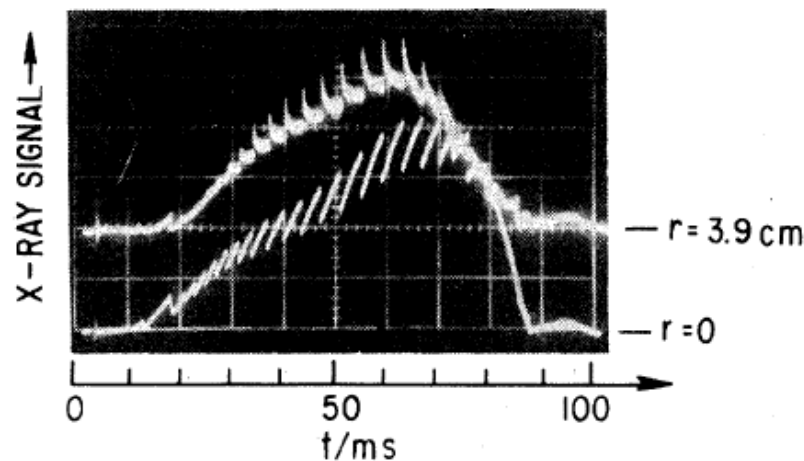
Studies of Internal Disruptions and $m = 1$ Oscillations in Tokamak Discharges with Soft-X-Ray Techniques*

S. von Goeler, W. Stodiek, and N. Sauthoff

Plasma Physics Laboratory, Princeton University, Princeton, New Jersey 08540

(Received 11 July 1974)

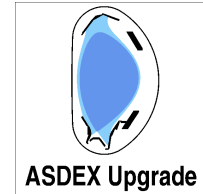
Fluctuations in x-ray intensity from the ST tokamak show a characteristic sawtooth behavior. This behavior is identified as an internal disruption. The internal disruptions are preceded by growing sinusoidal $m=1$, $n=1$ oscillations. The properties of these oscillations are compared with predictions for the $m=1$ internal kink mode.



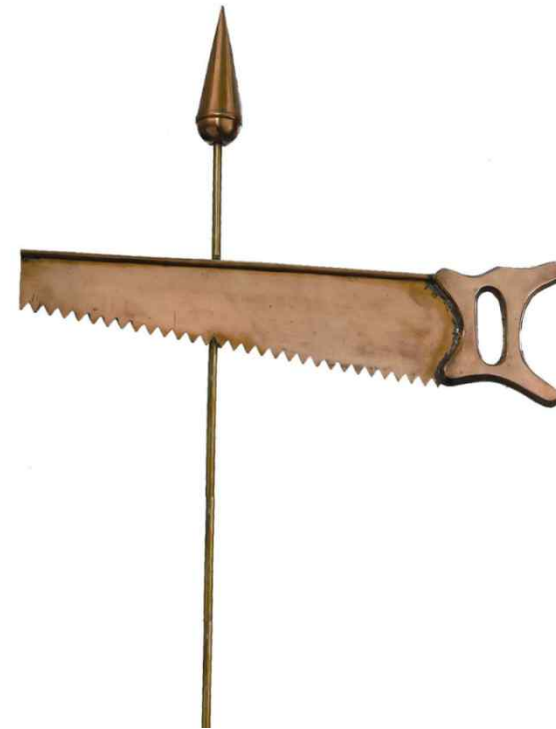
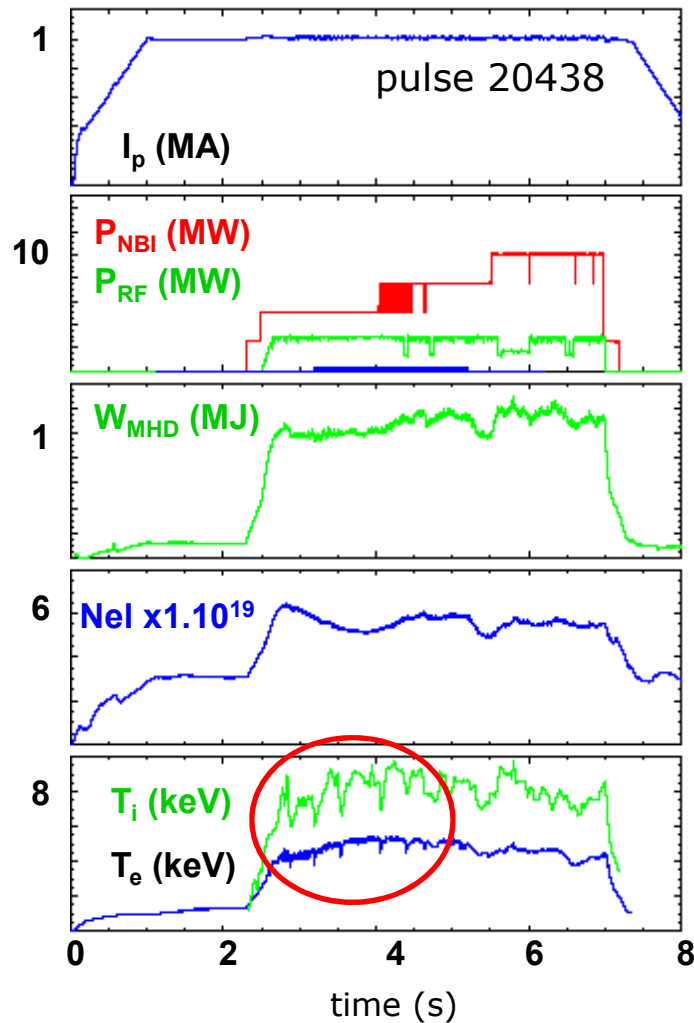
of the plasma electrons and consists predominantly of the recombination-radiation continuum of the partly ionized oxygen and iron impurities.¹ The radiation intensity is therefore a function of the electron density and temperature and of the impurity concentration. The x-ray fluctuations are caused by a fluctuation in either of these quantities, but predominantly by temperature fluctuations.

The oscillograms of the x-ray emissions, shown in Fig. 1, are typical for high-density discharges in the ST tokamak. The traces exhibit a "sawtoothlike" oscillation. The sawtooth is "inverted," showing a fast rise and a slow exponential drop,

Non-linear Plasma Activity



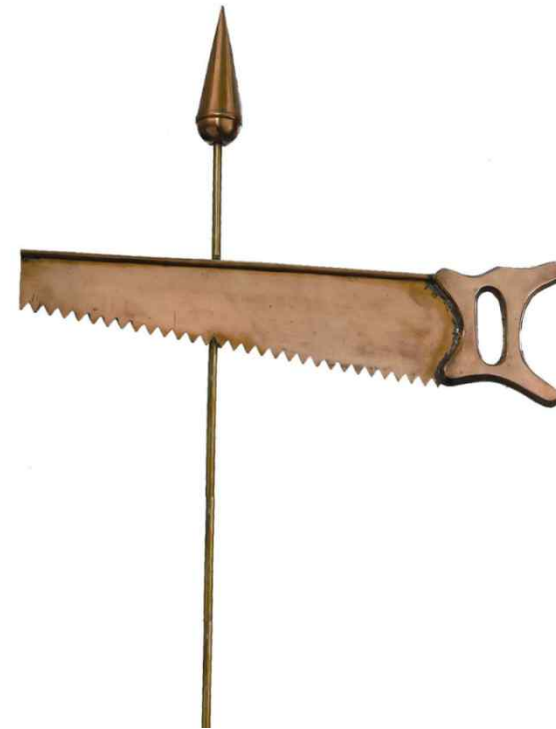
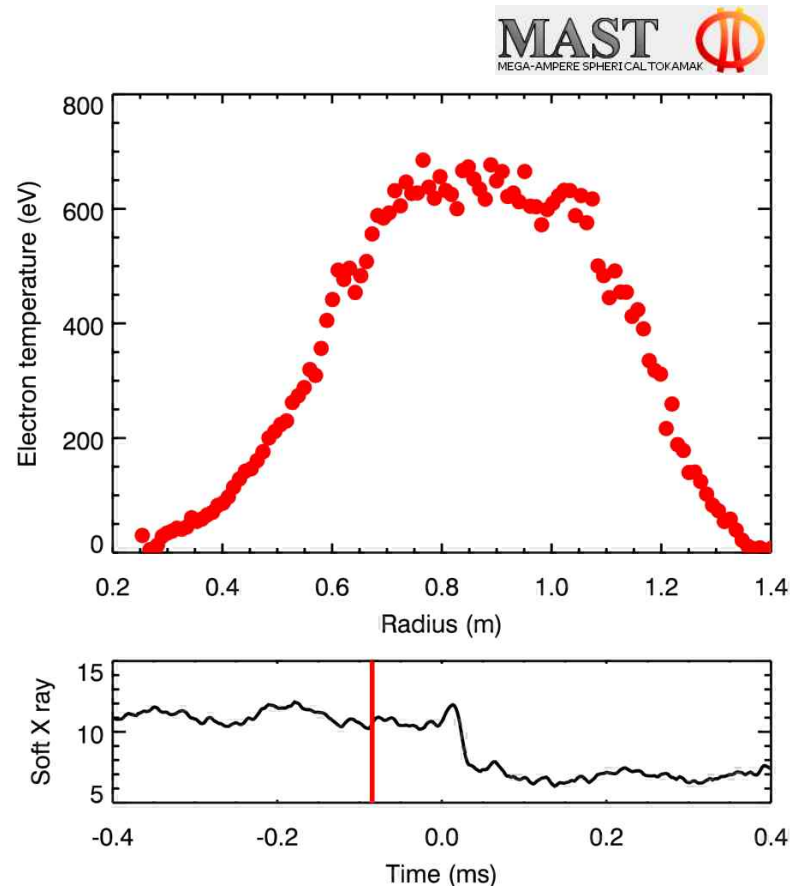
• Sawtooth



- nonlinear low- n internal mode
- internal (minor) disruption
- enhanced energy transport in the plasma centre

Non-linear Plasma Activity

- Sawtooth



IT Chapman et al, PRL, 2010

Non-linear Plasma Activity

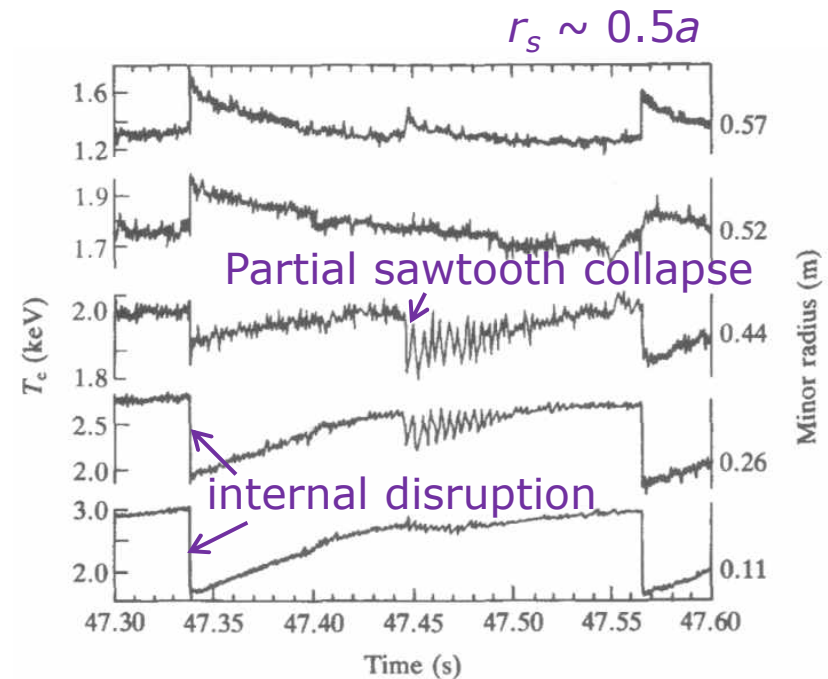
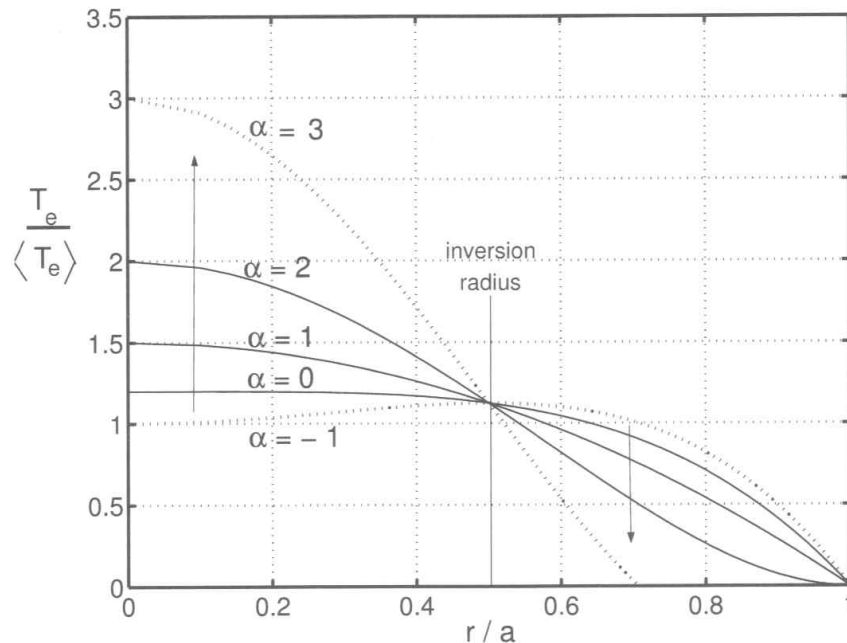
- **Sawtooth**

- It occurs so commonly that its presence is accepted as a signal that the tokamak is operating normally.
- Important type of plasma non-linear activity
 - Decreasing the thermal insulation
 - Key to understanding the disruptive instability
- Consisting of periodically repeated phases of
 - slow temperature rise at the centre of the plasma column
 - fast drop ($m = 1, n = 1$ oscillatory MHD modes oscillation precursors observed before the drop)

Non-linear Plasma Activity

- **Sawtooth**

- Inversion radius (r_s): when central temperature drops and flattens, the temperature decreases inside the radius and increases directly beyond it.

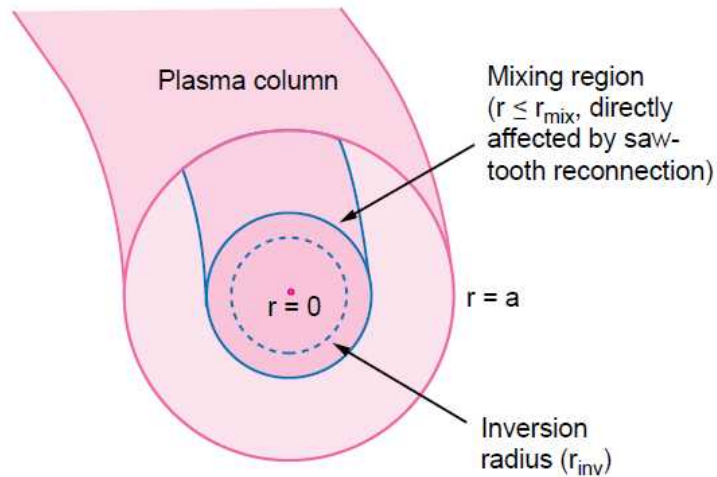


$$T_e = T_{e0} \left[1 - \alpha y - (1 - \alpha) y^2 \right] \quad T_{e0} = 6 \langle T_e \rangle / (5 - \alpha)$$

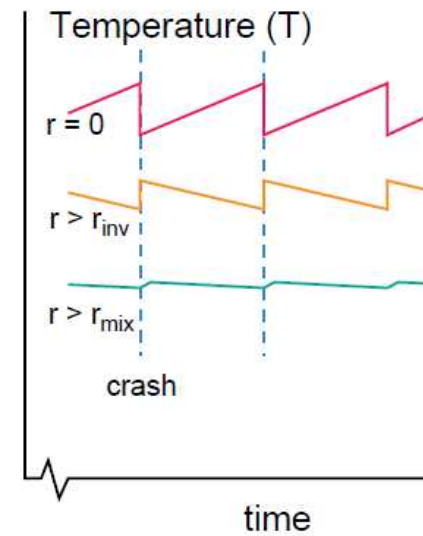
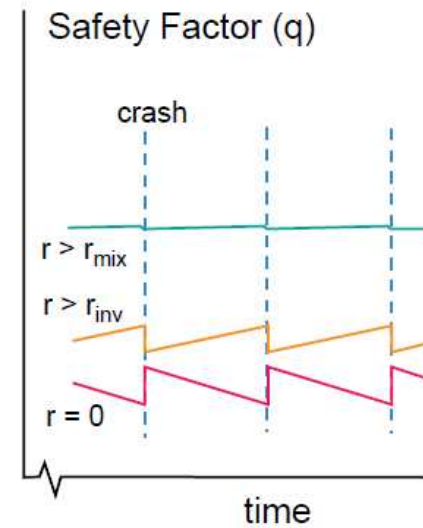
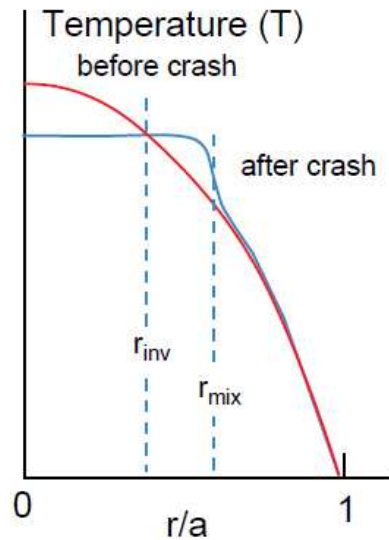
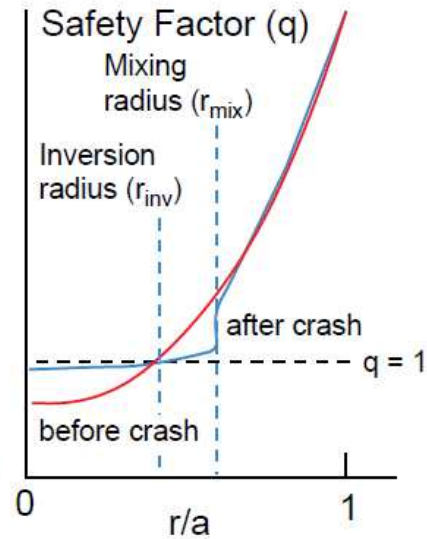


Non-linear Plasma Activity

• Sawtooth



ITER Physics Basis NF (1999)



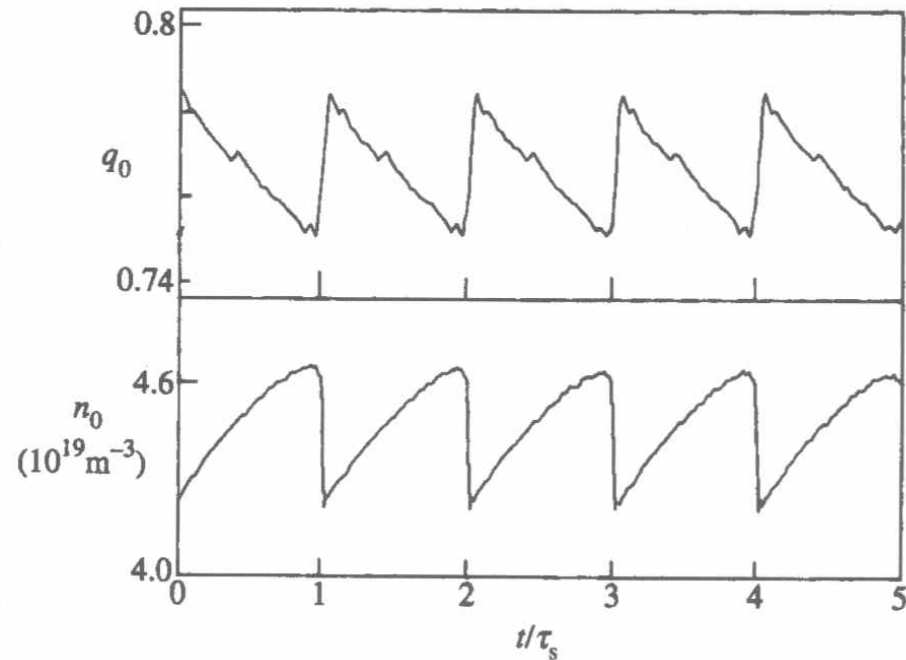
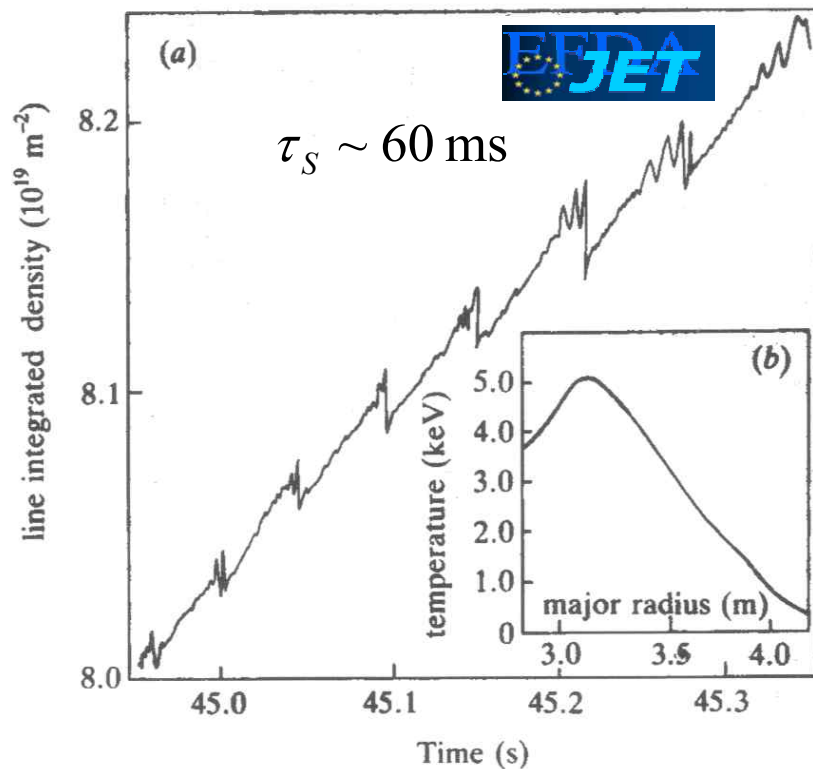
Non-linear Plasma Activity

- Sawtooth

- $\Delta T_e \sim 40\%$, $\Delta q_0 \sim 4\%$, $\Delta n_0 \sim 9\%$



TEXTOR
(H. Soltwisch et al, APS (1987))

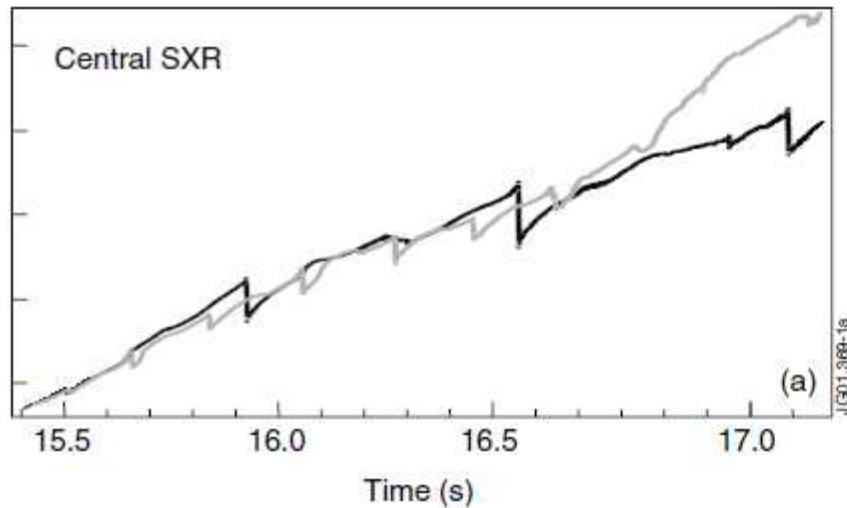


- Simple semi-empirical scaling for the period of sawtooth oscillations

$$\tau_S \approx 10^{-2} R^2 T_e^{3/2} / Z_{\text{eff}}$$

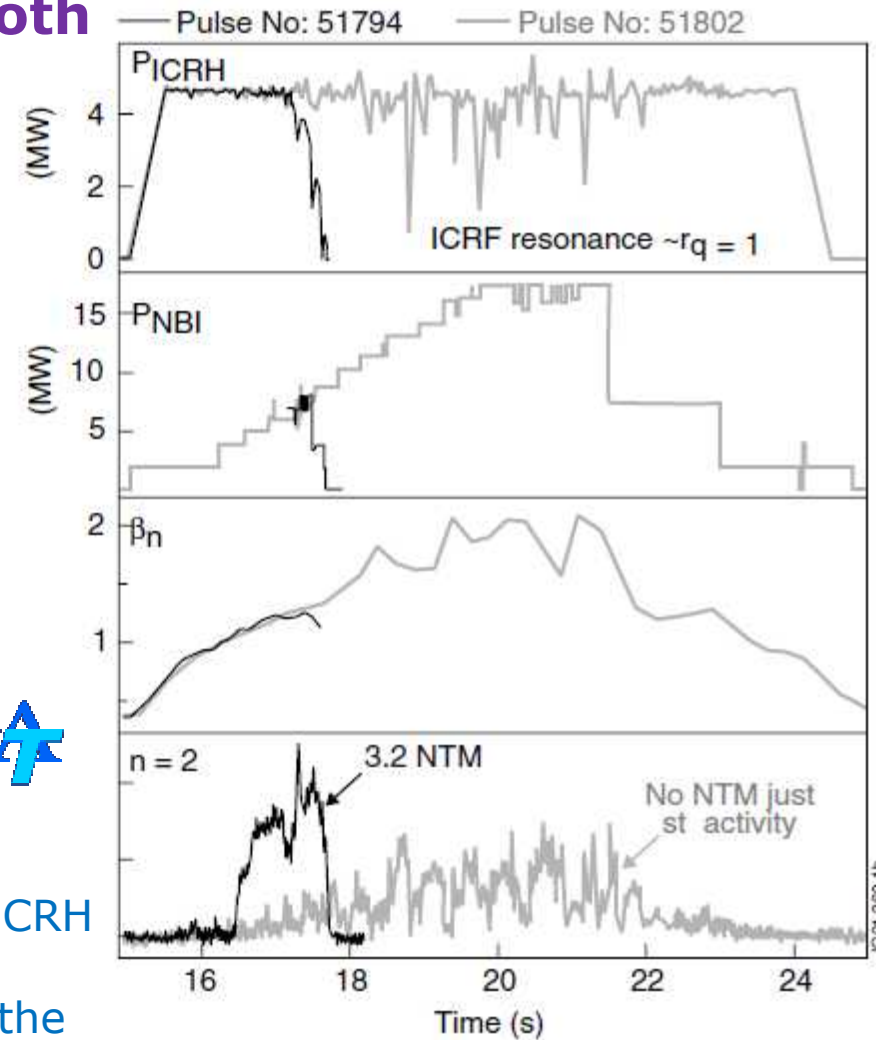
Non-linear Plasma Activity

- NTM triggered by Sawtooth



EFDA
JET

- Increased sawtooth period due to stabilisation by fast ions produced by ICRH leads to the triggering of $n = 2$ NTM activity which causes a termination of the discharge.



Non-linear Plasma Activity

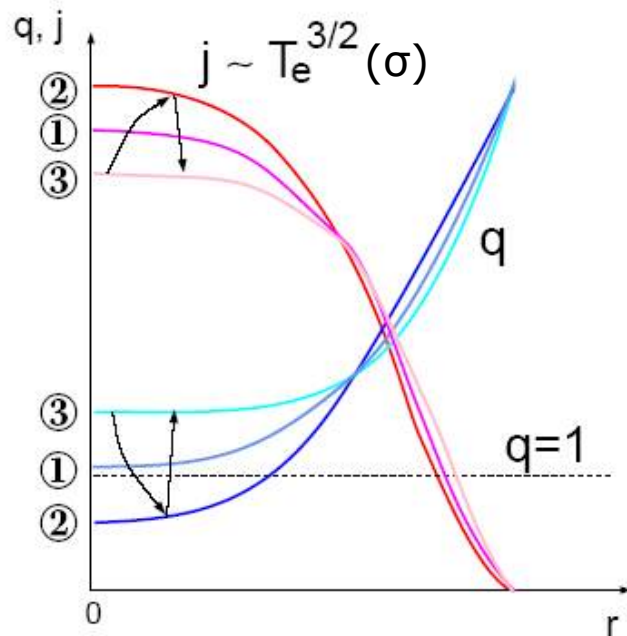
- **Sawtooth**

- Why the sawtooth oscillation should occur at all has not yet been explained.
- Two instabilities are required to drive the process
 - abrupt collapse
 - ramp phase

Non-linear Plasma Activity

- **Sawtooth**

- Kadomtsev model

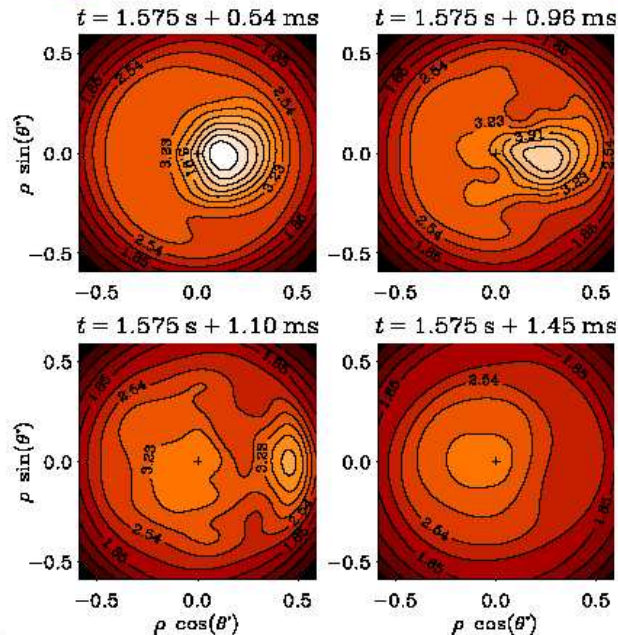
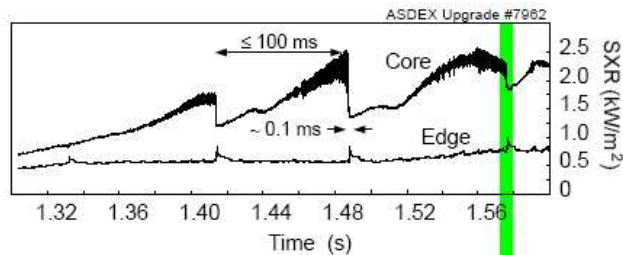


1. $T(0)$ and $j(0)$ rise due to ohmic heating (slower phase, resistive time scale)
2. $q(0)$ falls below 1, $q(r_s) = 1$
→ kink instability ($m/n=1/1$) grows
3. Fast reconnection event:
 T, n flattened inside $q = 1$ surface
 $q(0)$ rises slightly above 1
kink stable

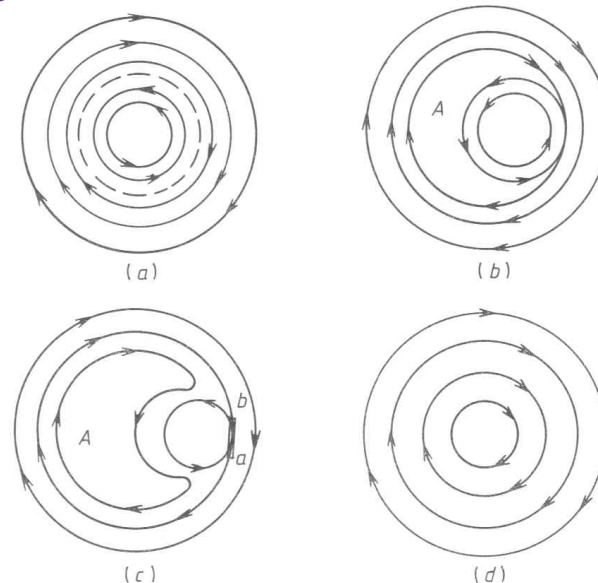
Non-linear Plasma Activity

- **Sawtooth**

- Kadomtsev model



- (a) auxiliary transverse field $B_* = B_\theta - (r/R)B_T$ (different direction of magnetic lines relative to the surface with $B_* = 0$)
- (b) contact of surfaces with oppositely directed fields B_*
- (c) reconnection of the current layer ab due to finite plasma conductivity. A moon-like island A formed due to the reconnection
- (d) final result of reconnections: auxiliary magnetic field is unidirectional

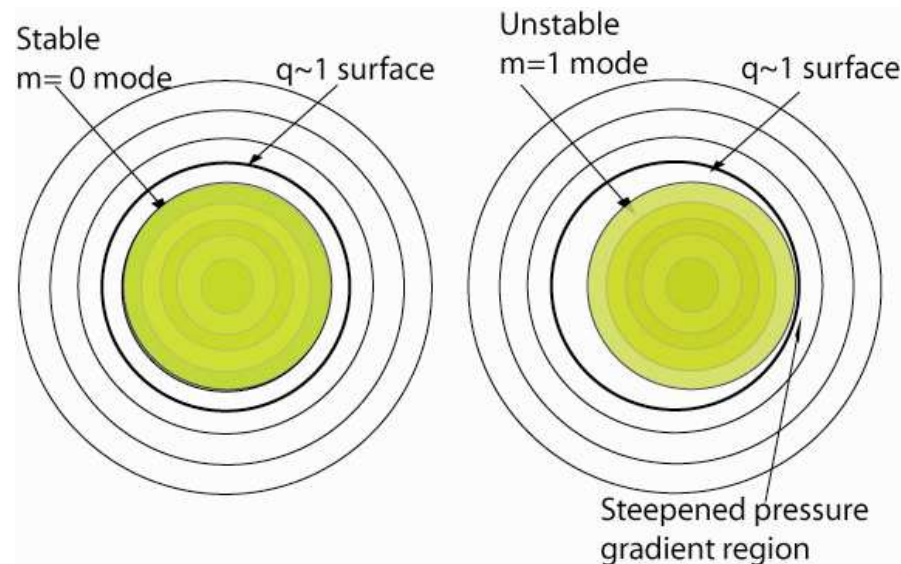


Non-linear Plasma Activity

- **Sawtooth**

- Kadomtsev model

- (a) auxiliary transverse field $B_* = B_\theta - (r/R)B_T$
(different direction of magnetic lines relative to the surface with $B_* = 0$)
- (b) contact of surfaces with oppositely directed fields B_*
- (c) reconnection of the current layer ab due to finite plasma conductivity. A moon-like island A formed due to the reconnection
- (d) final result of reconnections: auxiliary magnetic field is unidirectional



Non-linear Plasma Activity

- **Sawtooth**

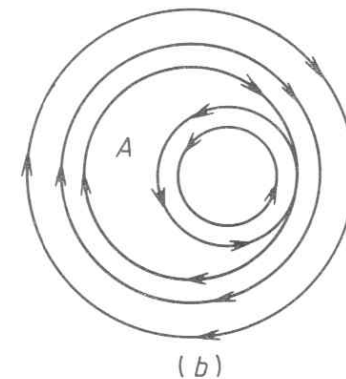
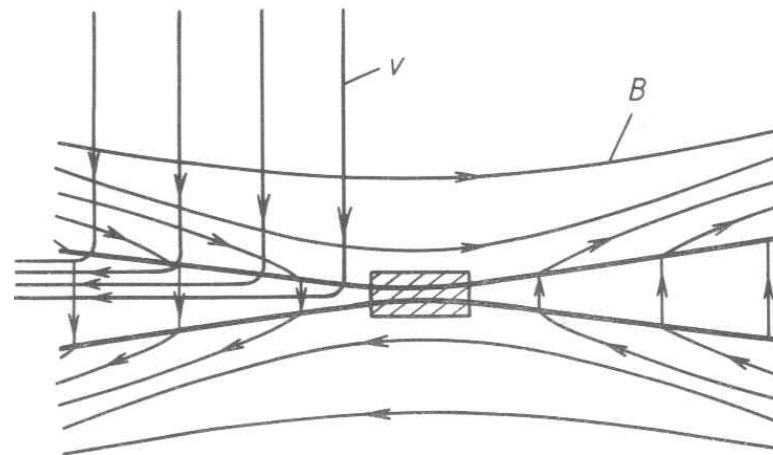
- Reconnection of the magnetic field lines: Sweet-Parker model
 1. Magnetic fields are pushed together by flows into a narrow region. In the flow regions the resistivity is low and hence the magnetic field is frozen in the flow. The two regions are separated by a current sheet (the reversal of the magnetic field requires a current to flow in the thin layer separating them). Within this layer resistive diffusion plays a key role.
 2. As the two regions come together the plasma is squeezed out along the field lines allowing the fields to get closer and closer to the neutral sheet.
 3. At some stage the field lines break and reconnect in a new configuration at a magnetic null-point, X . The large stresses in the acutely bent field lines in the vicinity of the null-point result in a double-action magnetic 'catapult' that ejects plasma in both directions, with velocity of $O(v_A)$. This in turn allows plasma to flow into the reconnection zone from the sides.

Non-linear Plasma Activity

- **Sawtooth**

- Reconnection of the magnetic field lines: Sweet-Parker model

1. The field diffuses into plasma and magnetic lines reconnect.
2. A kind of 'catapult' of strained magnetic lines is formed.
3. It throws out the plasma from the layer into the moon-like region *A* of the magnetic island (b)

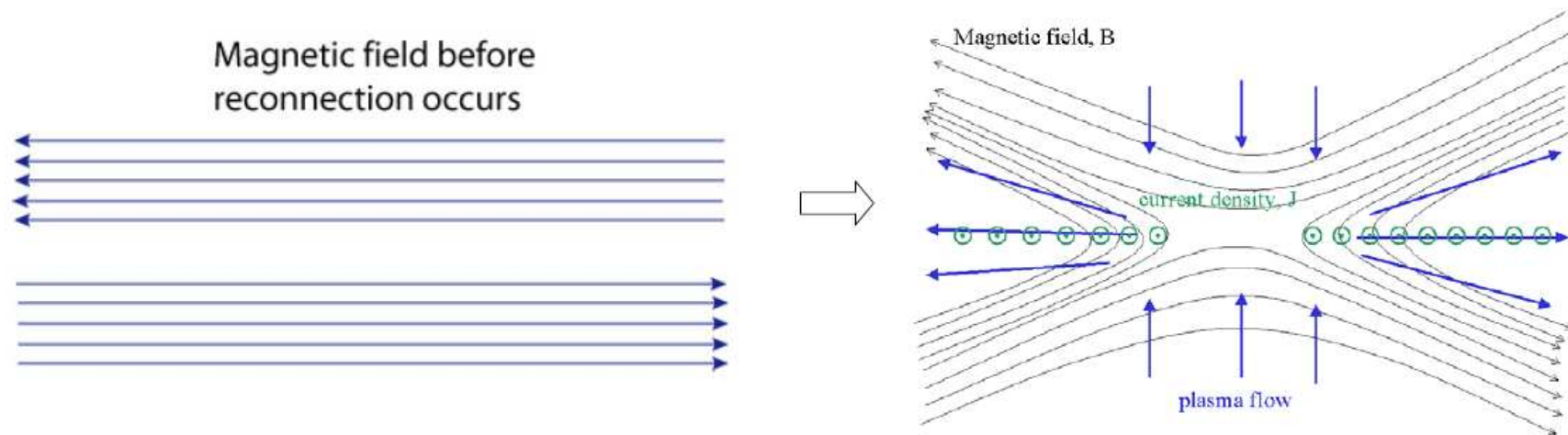


Non-linear Plasma Activity

- **Sawtooth**

- Reconnection of the magnetic field lines: Sweet-Parker model

1. The field diffuses into plasma and magnetic lines reconnect.
2. A kind of 'catapult' of strained magnetic lines is formed.
3. It throws out the plasma from the layer into the moon-like region A of the magnetic island (b)



Non-linear Plasma Activity

- **Sawtooth**

- Kadomtsev model

Shortcomings 1: collapse time for the disruption orders of magnitude longer than observed

$$\tau_c = \omega^2 / \xi_{\perp} \quad \text{collapse time } (\omega: \text{island width})$$

$$\xi_{\perp} = \frac{\eta}{\mu_0} = \frac{m_e}{\mu_0 e^2 n_e \tau_e} = 1.025 \times 10^8 \ln \Lambda / T_e^{3/2} \approx 4.4 \times 10^{-2} T_e^{3/2} \quad \text{magnetic diffusivity}$$

Ex) $\tau_c \sim 10$ ms at $\omega = 1$ cm, $T_e = 3$ keV

JET: $\tau_c = 50\text{-}200$ μs but Kadomtsev model gives $\tau_c \geq 10$ ms

→ If the collapse is associated with a magnetic rearrangement an explanation of its rapidity was required.

Non-linear Plasma Activity

- **Sawtooth**

- Kadomtsev model

- Shortcomings 2: no precise specification for the occurrence of a disruption

- Shortcomings 3: could not reproduce the sharp spikes on the disruption profile and that at the outset of the disruption the island size was much too small

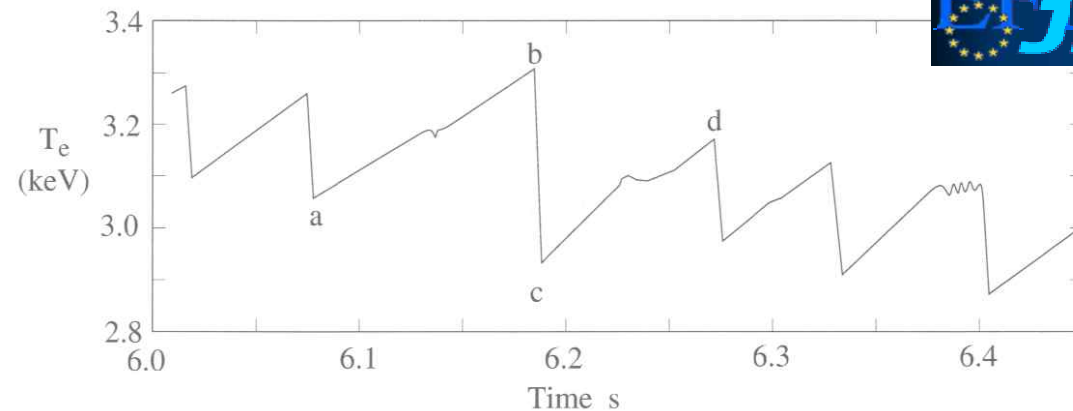
- Shortcomings 4: sometimes precursors are absent or lacking in experiments as is the case with the large amplitude oscillations known as 'giant' or 'compound' sawteeth

Non-linear Plasma Activity

- **Sawtooth**

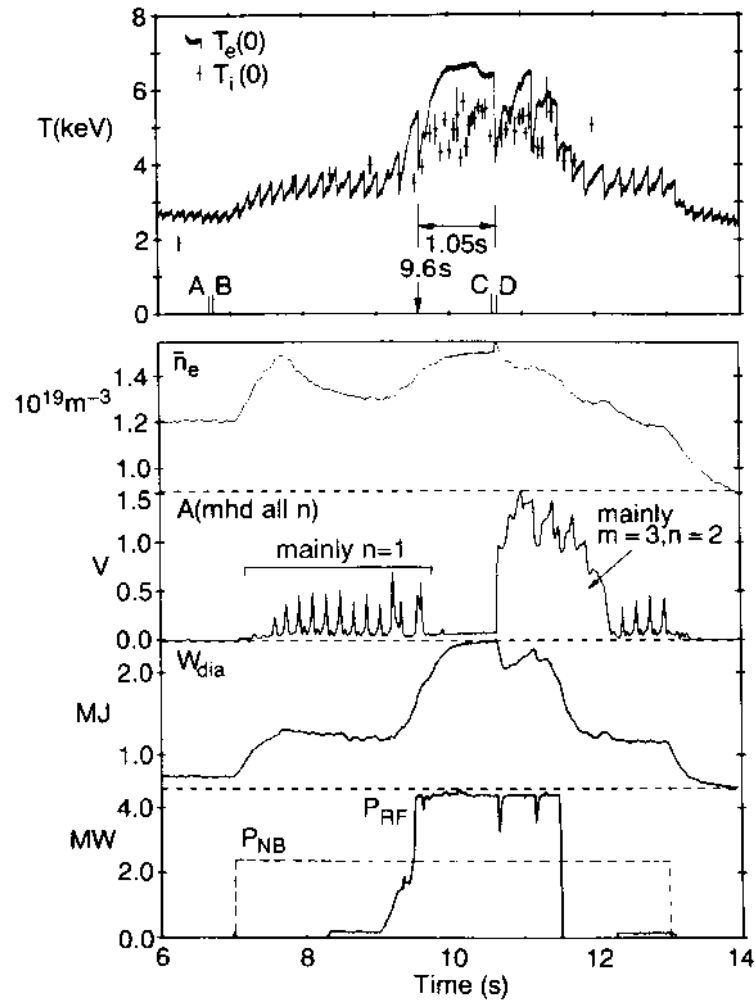
- Kadomtsev model

Shortcomings 5: existence of 'double' sawteeth with a longer and sometimes erratic period and a larger amplitude – requiring a hollow current profile with two $q = 1$ surfaces



Non-linear Plasma Activity

• Monster Sawtooth

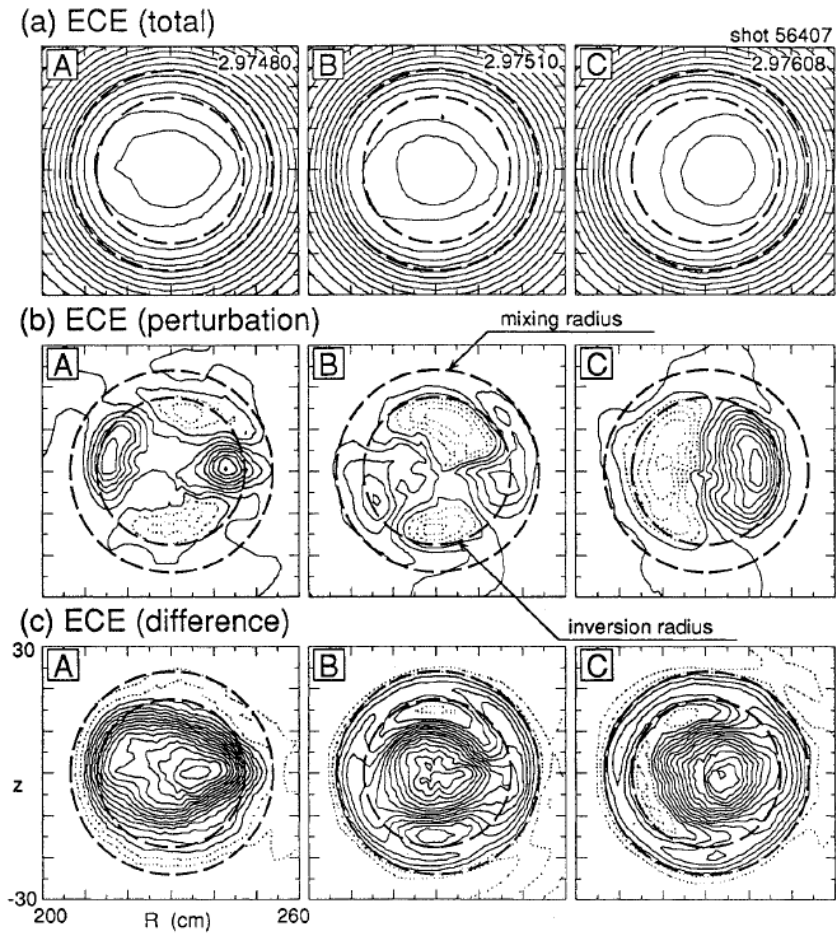
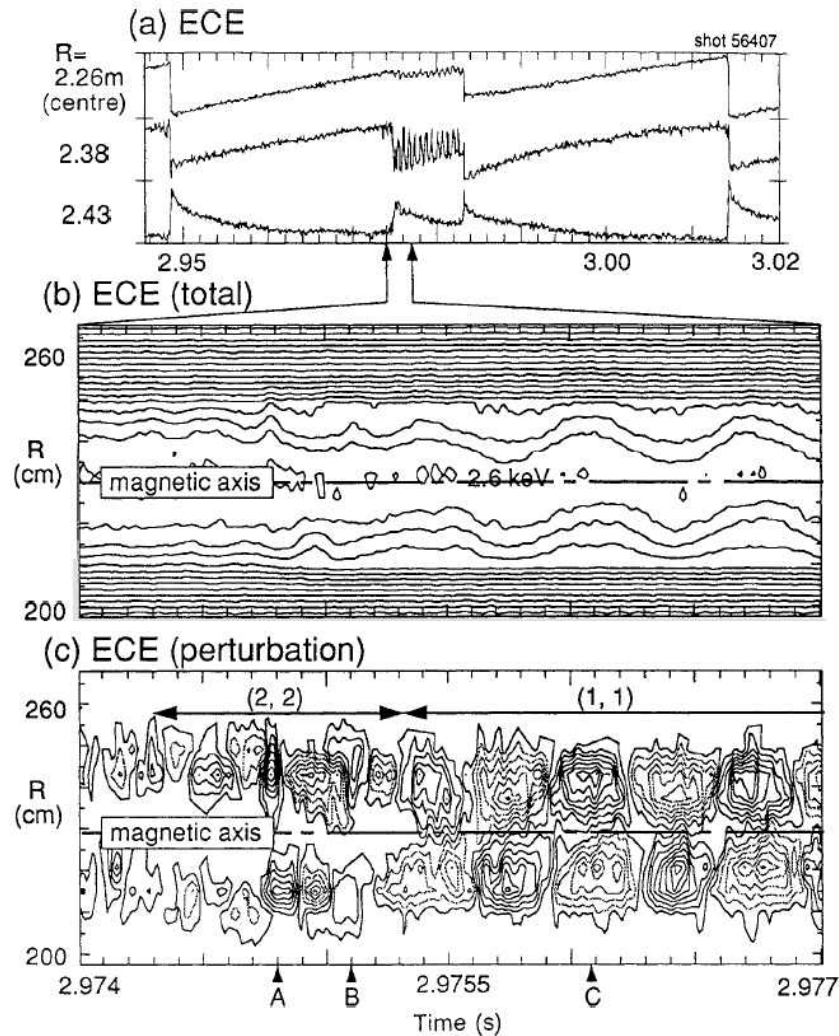


- No low (m,n) number coherent MHD activity observed during the temperature saturation phase
- ICRH and/or NBI above 5 MW
- Possibly due to stabilisation of the $m = 1$ instability by fast ions

*D. J. Campbell et al, PRL **60** 2148 (1988)*

Non-linear Plasma Activity

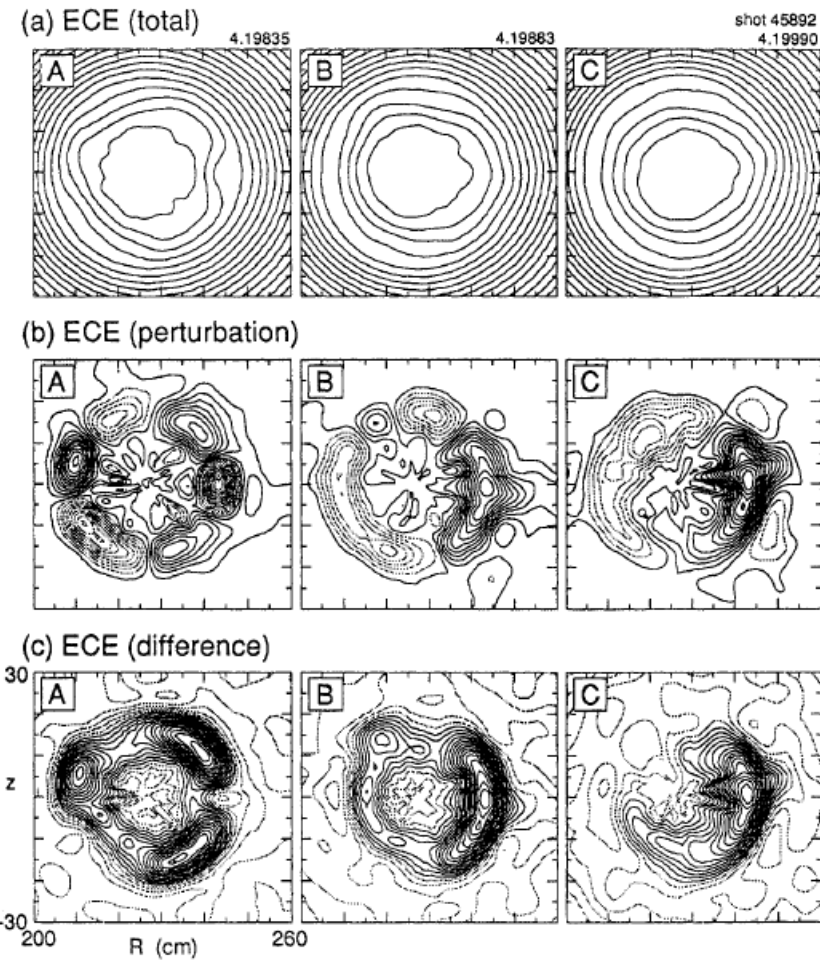
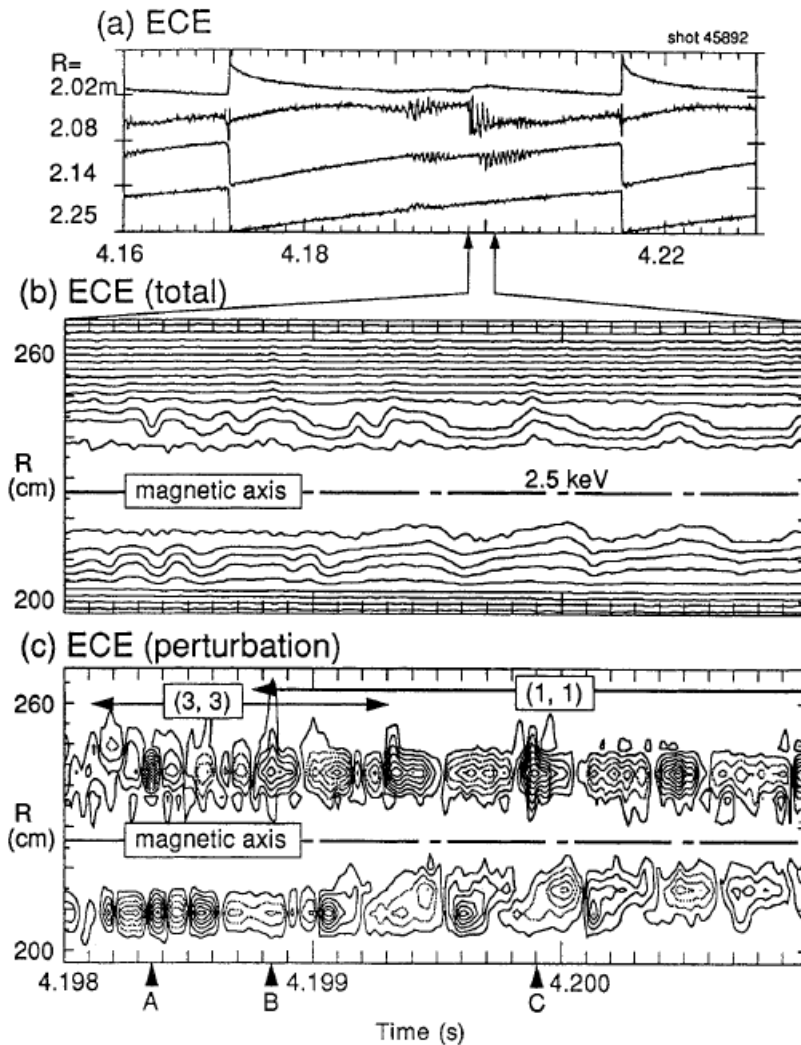
- Partial crash by higher modes



Y. Nagayama et al, NF 36 521 (1996) 47

Non-linear Plasma Activity

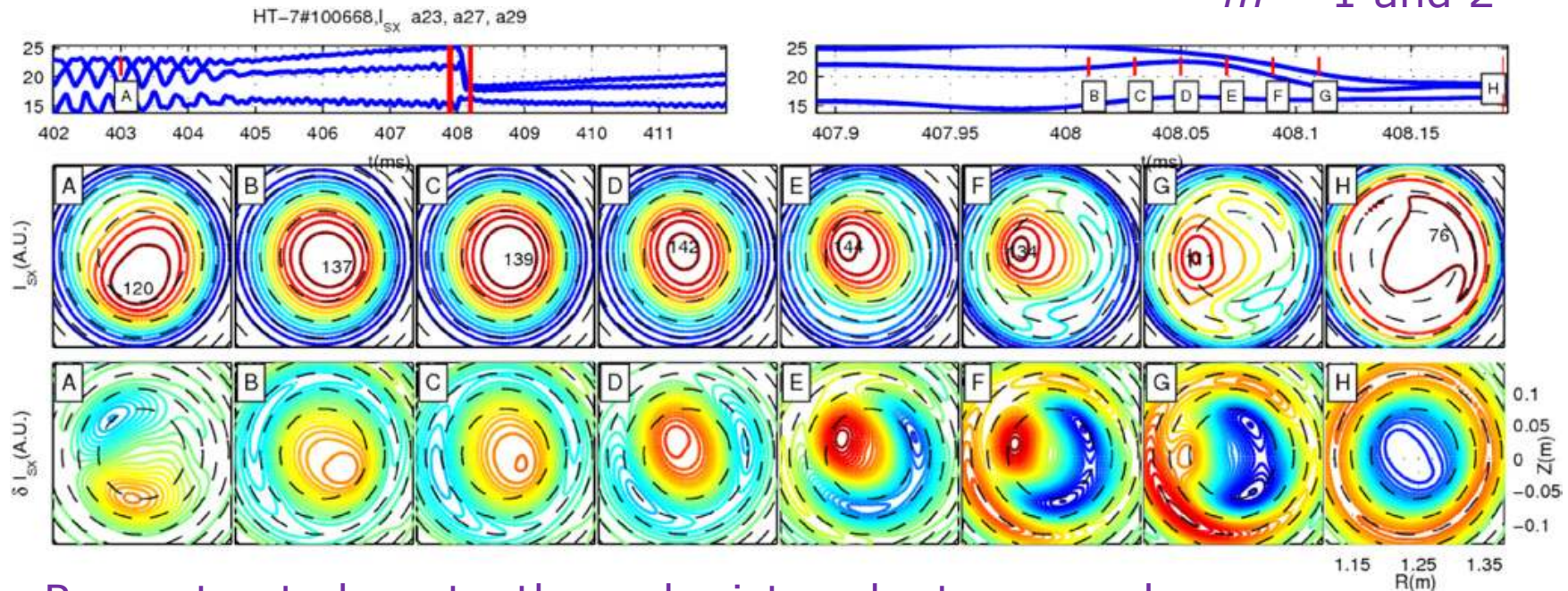
- Partial crash by higher modes



Non-linear Plasma Activity

- Partial crash by higher modes

$m = 1$ and 2



- Reconstructed sawtooth crash picture by tomography:
line-integrated soft-x-ray signals at 3 chords,
the contour plot of the reconstructed local emission intensities profile from the total signals,
the contour plot of the reconstructed perturbation of the local emission intensities from the
perturbation signals extracted by the SVD method

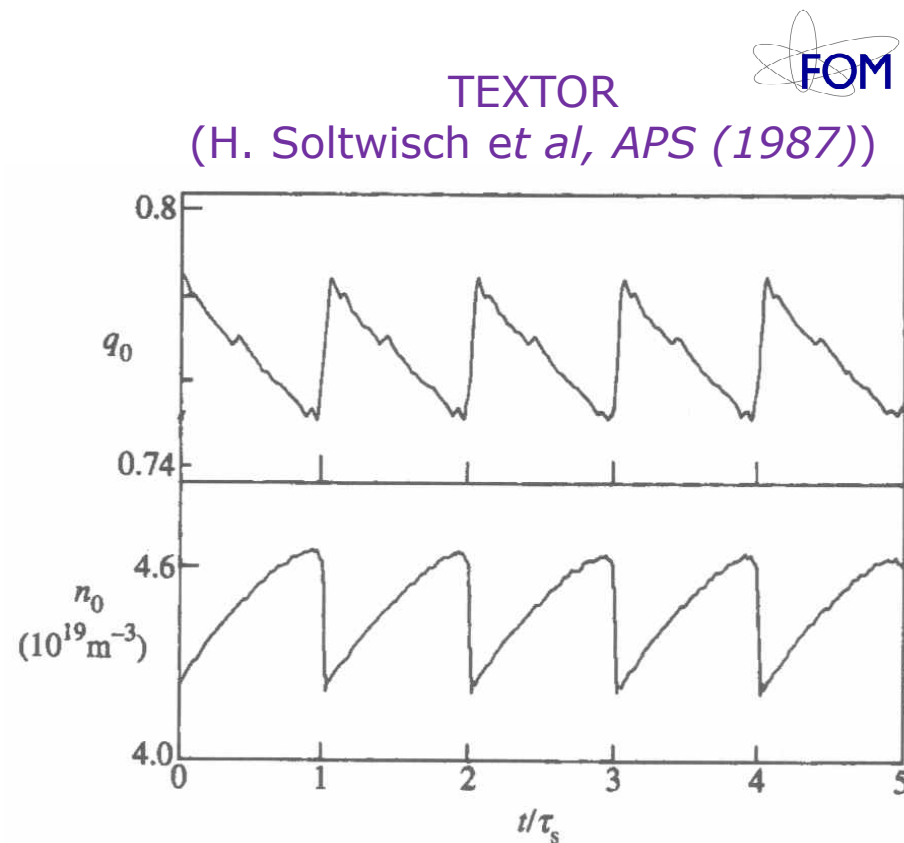
Youwen Sun et al, PPCF 51 065001 (2009)

Non-linear Plasma Activity

- **Sawtooth**

- Kadomtsev model

Shortcomings 6: q_0 remains below unity in many experiments



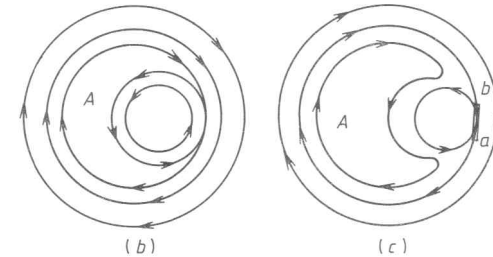
$q_0 < 1$ (~ 0.7) during all the sawtooth period
(F. M. Levinton *et al*, PRL **63** 2060 (1989))

Non-linear Plasma Activity

• Sawtooth

- Phase of the sharp temperature profile flattening (internal disruption)

1. What is the trigger of the internal disruption (type of instability)?
2. How does the disruption develop?
3. What is the time of disruption?

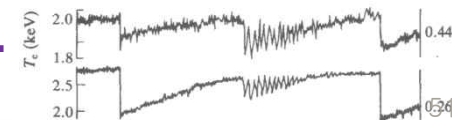


- Internal $m = 1/n = 1$ snake

- In some cases, instability when β_p inside r_s exceeds a certain critical value

- Every force tube 'catapulting' into A may drastically perturb plasma and create MHD-turbulence. If a turbulent zone is formed in A , then the B_* mean value may disappear due to mixing of magnetic lines. Then there is no force that would 'press' the internal core to the magnetic surface with the inverse magnetic field.

→ partial (incomplete) reconnection



Non-linear Plasma Activity

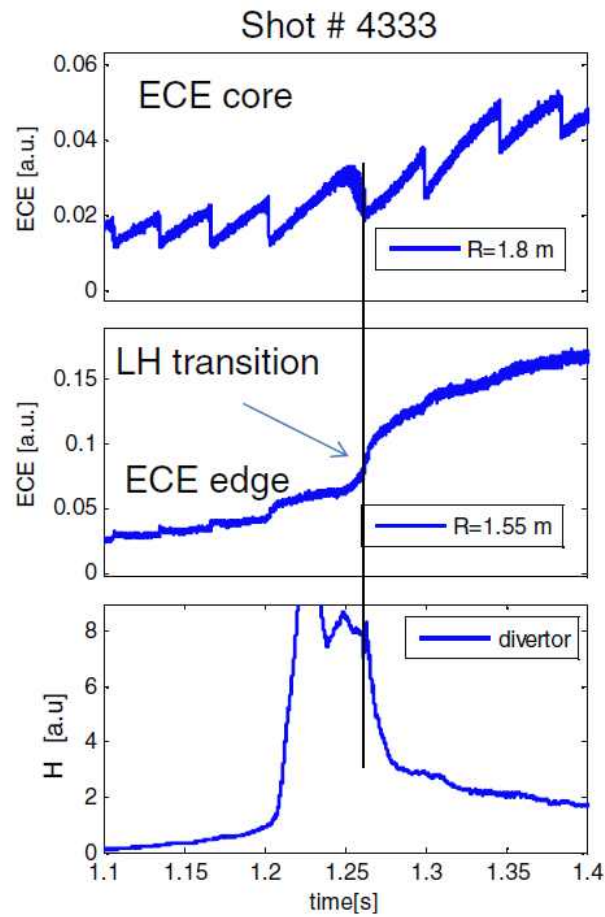
- **Sawtooth**

- Stochasticity of the magnetic field lines may appear due to the toroidicity which violates the ideal helical symmetry.
 - change significantly the resistivity value inside the current layer
 - electron does not return back to the same point if after crossing the current layer, an anomalous skin-layer can develop.
 - significantly increasing the reconnection rate and makes it close to the observed one at the fastest internal disruptions.

Non-linear Plasma Activity

- **Sawtooth**

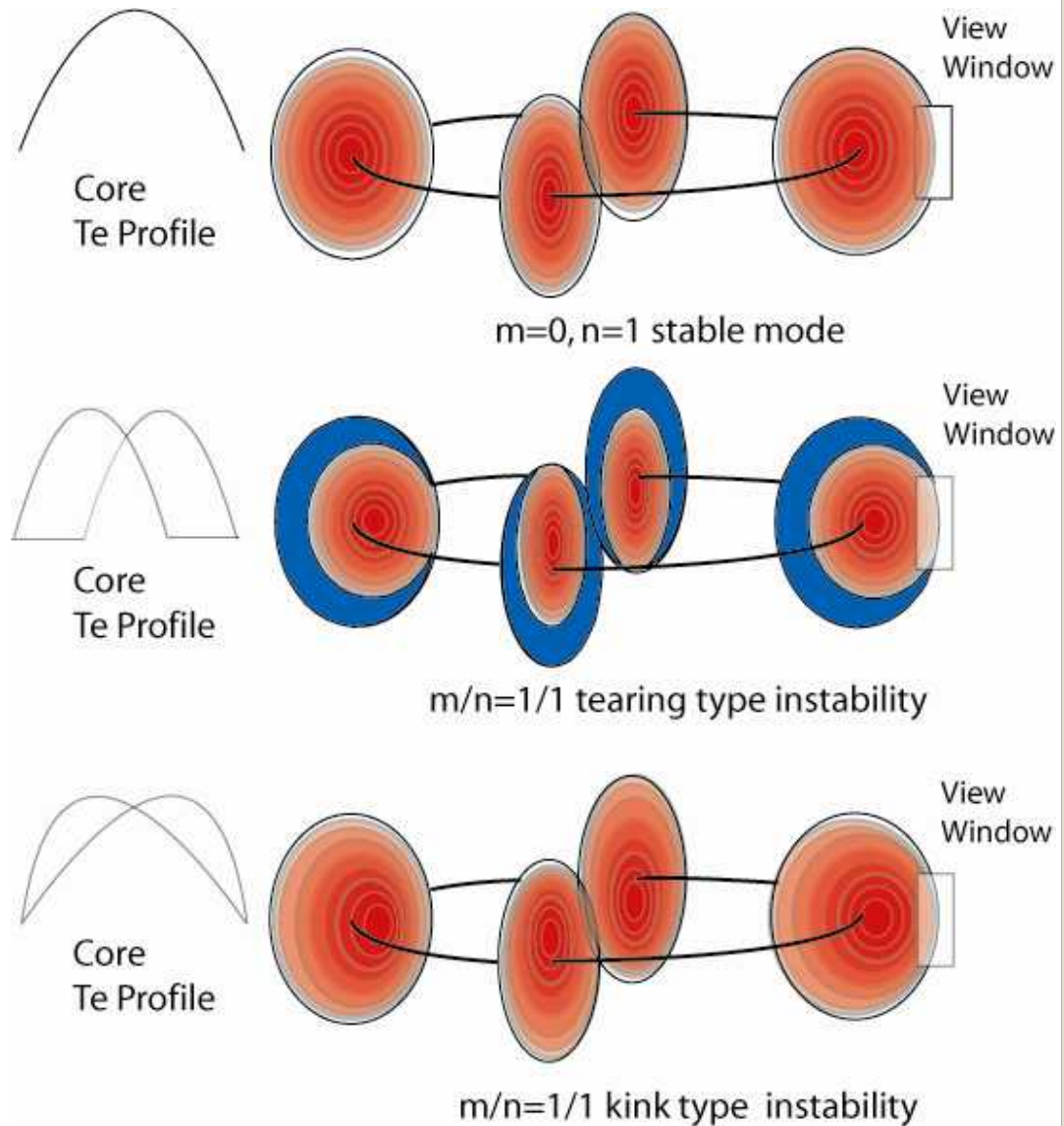
- Sawtooth triggered L-H transition



S.W. Yoon et al, NF 51 113009 (2011)

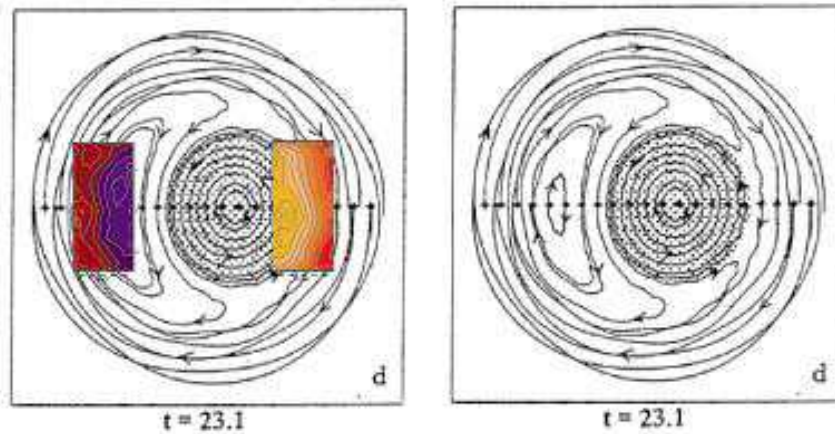
Sawtooth

- Stable $m/n=0/1$ mode in the initial stage
- $m/n=1/1$ mode develops as the instability grows (kink or tearing instability) and reconnection occurs
 - Tearing mode instability (slow evolution of the island/hot spot)
 - Kink mode instability (sudden crash)
- Reconnection time scale is any different in these two types?

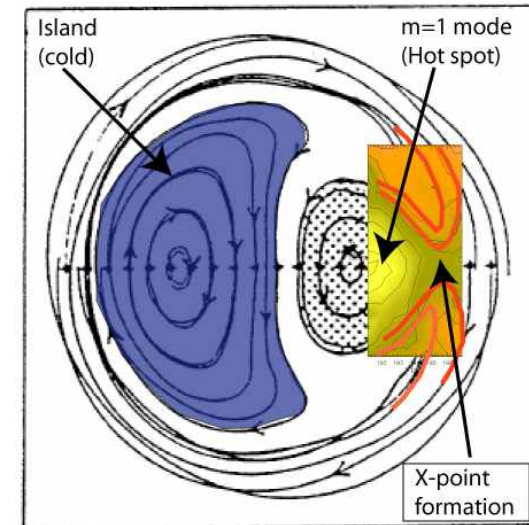
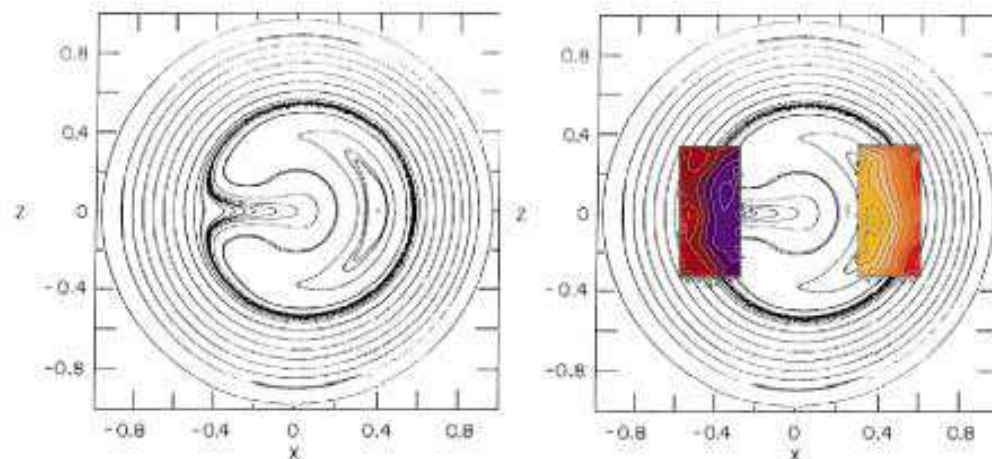


Sawtooth

- Comparison with the full reconnection model



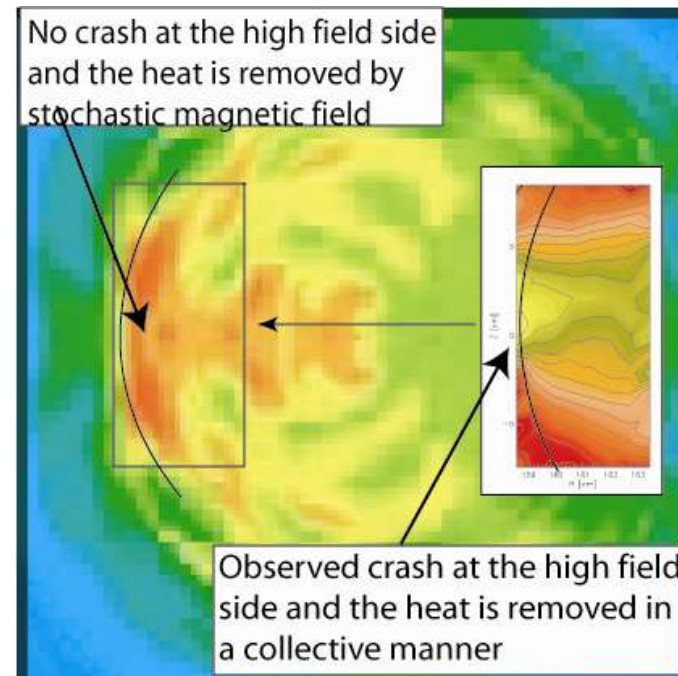
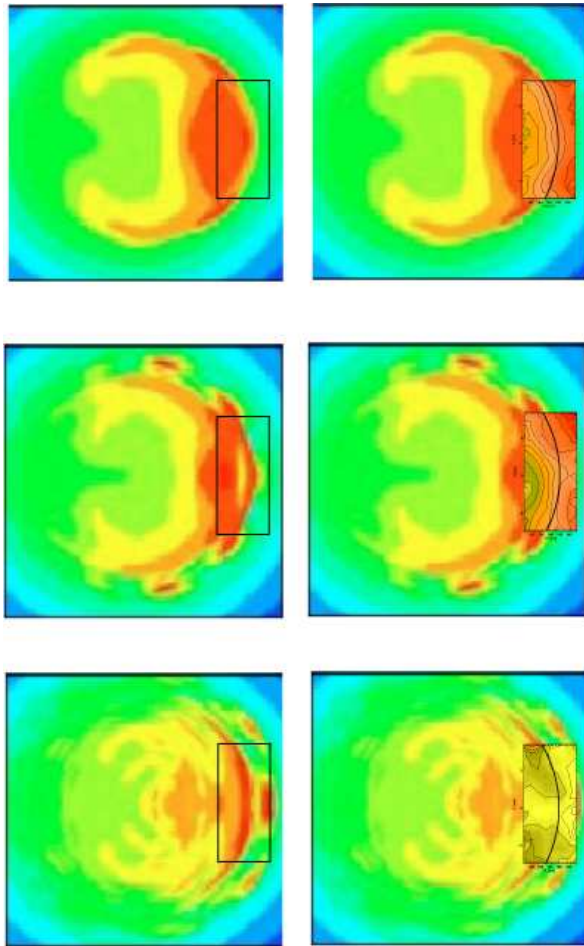
- Comparison with the quasi-interchange model



Comparison with the full reconnection model simulation result at the low field side

Sawtooth

- Comparison with the ballooning mode model

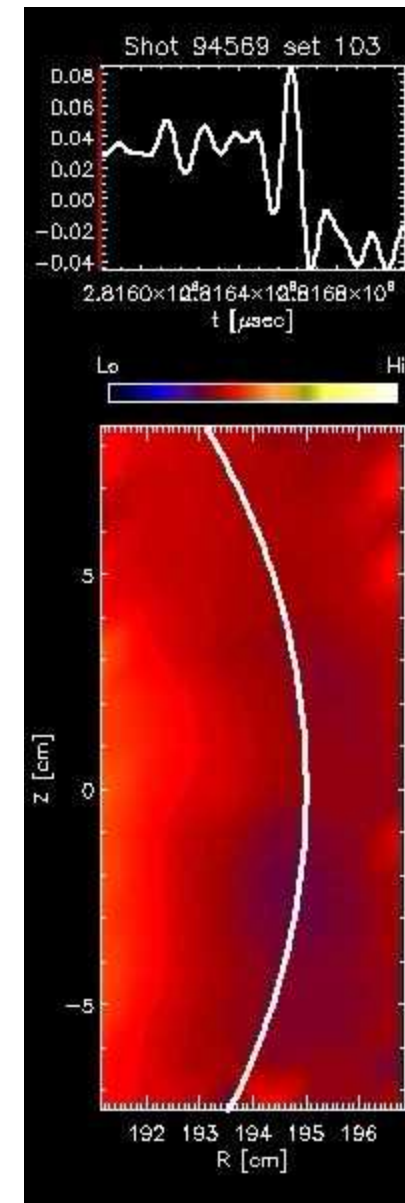
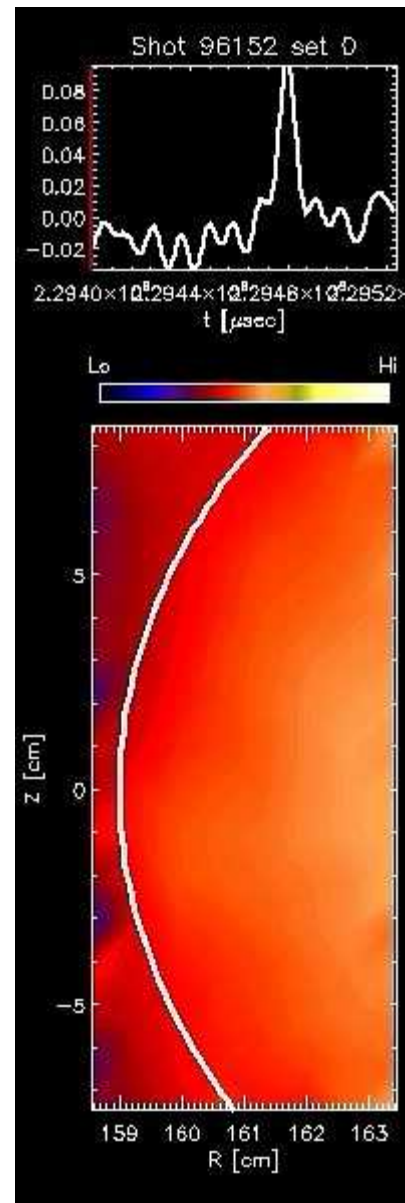


Comparison with the Ballooning model simulation result at the high field side

Low field side

Sawtooth

- 2-D ECE imaging diagnostic



H.K. Park
(UNIST)

References

- R. Goldston and P. H. Rutherford, Ch. 20 in "Introduction to Plasma Physics", Institute of Physics Publishing, Bristol and Philadelphia, 1995
- Wolfgang Suttrop, "Experimental Results from Tokamaks", IPP Summer School, IPP Garching, September, 2001